

RESEARCH

Open Access



Quantifying the impacts of spatiotemporal land use and land cover changes on soil loss across agroecologies and slope categories using GIS and RUSLE model in Zoa watershed, southwest Ethiopia

Ginjo Gitima^{1*} , Menberu Teshome² , Meseret Kassie¹  and Monika Jakubus³ 

Abstract

Background Soil erosion in Ethiopian highlands is highly consistent with land use/land cover (LULC) changes that are associated with deforestation and a decline in biodiversity. However, identifying soil erosion-prone areas and quantifying soil loss in rugged terrains and various agroecologies due to LULC changes have not been dedicated to scientific studies. Therefore, we quantified the impacts of spatiotemporal LULC changes on soil loss across agroecologies and slope categories using GIS and RUSLE model from 1985 to 2021 in Zoa watershed, southwest Ethiopia. Moreover, prioritizing erosion severity risks at sub-watersheds and quantifying temporal sediment yield is essential for better conservation planning. Landsat images, rainfall, Digital Elevation Model, and soil data were obtained from field observations and secondary sources.

Results Bareland and farmland have been expanding at the expense of other land use types. The annual soil loss in the watershed ranged from 0 to 113.21 t ha⁻¹ year⁻¹, 0 to 163.16 t ha⁻¹ year⁻¹, and 0 to 194.58 t ha⁻¹ year⁻¹ with a mean annual soil loss of 21.07, 29.35 and 40.93 t ha⁻¹ year⁻¹ in 1985, 2000, and 2021, respectively. Among LULC classes, the highest soil loss was generated from bareland (31.73 t ha⁻¹ year⁻¹) and farmland (27.08 t ha⁻¹ year⁻¹) in 1985 later upsurged to 35.52 t ha⁻¹ year⁻¹ and 59.91 t ha⁻¹ year⁻¹ in 2021, respectively, due to the maximum susceptibility of soil erosion risks from unprotected surfaces. The results also revealed that the lowland agroecology generated the highest mean soil loss of 24.05 t ha⁻¹ year⁻¹ in 1985, 39.74 t ha⁻¹ year⁻¹ in 2000, and increased to 57.55 t ha⁻¹ year⁻¹ in 2021. Considering the slope categories, the highest and most excruciating soil loss was engendered from steep (35.55–60.78 t ha⁻¹ year⁻¹) and very steep (52.48–72.69 t ha⁻¹ year⁻¹) slope terrains during 1985–2021. The northwestern part of the watershed is the most erosion-prone area which is now expanding to the central and western parts of the watershed. The sediment yield increased at the fastest rate at the watershed outlet, from 39.3% in 1985 to 94.26% in 2021.

Conclusions The results of this study indicated that the conversion of other LULC categories into farmland was the most detrimental to a watershed in terms of soil loss, which necessitates the implementation of appropriate soil and water conservation measures with effective design by considering spatial variability to reduce soil erosion hazards.

Keywords Soil erosion, RUSLE, Land use/land cover, Slope gradient, Tolerable soil loss, Soil conservation

*Correspondence:

Ginjo Gitima

ginjo.gitimo@bongau.edu.et

Full list of author information is available at the end of the article



© The Author(s) 2023. **Open Access** This article is licensed under a Creative Commons Attribution 4.0 International License, which permits use, sharing, adaptation, distribution and reproduction in any medium or format, as long as you give appropriate credit to the original author(s) and the source, provide a link to the Creative Commons licence, and indicate if changes were made. The images or other third party material in this article are included in the article's Creative Commons licence, unless indicated otherwise in a credit line to the material. If material is not included in the article's Creative Commons licence and your intended use is not permitted by statutory regulation or exceeds the permitted use, you will need to obtain permission directly from the copyright holder. To view a copy of this licence, visit <http://creativecommons.org/licenses/by/4.0/>.

Introduction

Soil degradation is one of the most serious environmental problems in the world (Tesfahunegn et al. 2014; Zhang et al. 2017; Teng et al. 2018; Lin et al. 2020) with a quantified count of 24 billion tons of top productive soil loss from the croplands on a global scale (Legese and Gelanew 2019). Soil erosion is the leading cause for the degradation of soil resources and the foremost environmental problem accounting for 56% of the world's land area (Gelagy and Minale 2016). In regional contrast, soil erosion is more dominant in developing countries (global south) than in developed countries due to various multifaceted spatiotemporal land use types and biophysical drivers interlinking to impact soil resources (Fenta et al. 2020). This is due to the largest number of people relying on land resources, the lack of proper land management measures, and the continuous expansion of cropland in developing countries including Africa (Borrelli et al. 2017; Haregeweyn et al. 2017). Similarly, different land use patterns in East Africa coincide with areas of high susceptibility to soil erosion hazards (Wynants et al. 2019; Fenta et al. 2020).

Among the East African countries, soil erosion is a severe problem in Ethiopia due to rapid changes in land use/land cover (LULC) types (Belay and Mengistu 2021). Consequently, Ethiopian highlands were mainly affected by sheet and rill erosion (Gashaw et al. 2019; Yesuph and Dagneu 2019) with the annual soil loss ranging from 200 to 300 t ha⁻¹ year⁻¹ (Gelagy and Minale 2016). Likewise, FAO (1986) appraised total soil loss at almost 1.5 billion tons per year from the whole landscape. Subsequently, the anticipated cost of soil loss effect was US\$1.9 billion between 1985 and 2010 in the country (FAO 1986). If the magnitude of soil erosion continues, the value-added in the agricultural sector will decline from 372 US\$ in 2010 to 162 US\$ in 2030 (Gashaw et al. 2019; Dinka 2020). The country also lost US\$1 billion per year because of soil erosion and it still upsets 50% of the croplands and 88% of the country's total inhabitants (Bekele et al. 2019). The soil erosion is highly consistent with spatiotemporal LULC dynamics (Messay 2011) as usually the alterations are associated with deforestation, a decline in biodiversity, and soil loss (Tsegaye 2019). In contrast, soil loss computed from conserved-land uses (37 t ha⁻¹ year⁻¹) is lower than that from adjacent non-conserved lands, i.e., 45 t ha⁻¹ year⁻¹ (Debie 2021). Likewise, the magnitude of soil loss varies across the country due to LULC changes, intrinsic soil features, slope terrains, and agroecological settings. For instance, the mean yearly soil losses (42.29 t ha⁻¹ year⁻¹, 45%) originated from cultivated land use class (Hurni et al. 2008; Amsalu and Mengaw 2014), which comprised a total soil loss of 23,400 million t (Tessema et al. 2020). Moreover, due to marginal agriculture

intensifications and inadequate conventional land management techniques, farmland experienced much more extreme soil erosion than grassland and forestland (Han et al. 2020). These hitches have led to declined productivity of land, poverty, unsustainability, and food insecurity (Adimassu et al. 2014; Yesuph and Dagneu 2019). For instance, in the highlands of Ethiopia yearly productive capacity is falling by 2.2% year⁻¹ (Tesfahunegn et al. 2014).

In the last four decades, many researchers developed and used soil erosion assessment models using geospatial technologies to quantify soil losses (e.g., Wischmeier and Smith 1978; Williams and Berndt 1977; Renard et al. 1994; Farhan et al. 2013; Pan and Wen 2014; Chang et al. 2016; Barriuso Mediavilla et al. 2017; Borrelli et al. 2017; Zhang et al. 2017; Teng et al. 2018; Alewell et al. 2019; Almouctar et al. 2021; Amellah and Morabiti 2021; Kuli-mushi et al. 2021a, b). However, the most universal and empirical-based models are USLE (Wischmeier and Smith 1978), MUSLE (Williams and Berndt 1977), and RUSLE (Revised Universal Soil Loss Equation) (Renard et al. 1994). The RUSLE is substantial to calculate the total and mean soil losses in a certain watershed. Due to its simplicity and compatibility with GIS, scholars have extensively and successfully used it to estimate soil erosion related to LULC changes depending on their study objectives and backgrounds (Gizachew 2015; Molla and Sisheber 2017; Tadesse et al. 2017; Tesfaye and Tibebe 2018; Kidane et al. 2019; Gashaw et al. 2019; Atoma et al. 2020; Dinka 2020; Fenta et al. 2020; Tessema et al. 2020; Bekele and Gemi 2020; Mengie et al. 2022), and these studies are confirmed in the context of Ethiopian.

Different scholars have quantified soil loss in different parts of Ethiopian highlands. To mention a few, the scholars focused on soil loss assessment and risk area (Amsalu and Mengaw 2014; Gelagy and Minale 2016; Tesfaye and Tibebe 2018; Bekele et al. 2019; Atoma et al. 2020; Girma and Gebre 2020; Tadesse et al. 2017; Tessema et al. 2020). Most of these studies assessed comprehensive soil loss estimation with inconsistent figures due to different LULC types in diverse terrains and agroecologies in various parts of the country. Other scholars conducted soil erosion estimation from each land use class without including major factors such as slopes, terrains, and agroecological settings (Belayneh et al. 2019; Bekele and Gemi 2020; Dinka 2020; Girmay et al. 2020). However, as far as the researchers' knowledge, soil loss in the Zoa watershed of the Omo-Gibe basin has not yet well-quantified. Studies conducted by Tebebu et al. (2010), Tesfaye and Tibebe (2018) and Yesuph and Dagneu (2019) suggested that the assessments of soil loss and its magnitude vary by location depending on the diverse land uses, population pressure, type, and susceptibility of the soils

to erosion, microclimate, the general terrain features, and agroecological variations of a given area. Since Ethiopia comprises various types of slope terrains, diverse agroecologies, and socioeconomic dynamics (Ewunetu et al. 2021), the timely site-specific study of soil loss by integrating RUSLE and geospatial technologies in dynamics of land uses can provide more insight into sustainable natural resource management decision-making.

As part of the southwestern Ethiopian highlands, Zoa watershed is a notable part of the Gibe-III and IV hydroelectric dams within the Omo-Gibe basin which needs a detail assessment of soil loss to sustain the benefits of these two dams. The rugged terrain features and a variety of LULC dynamics have caused soil erosion in the watershed. Moreover, the watershed has conspicuous forms of soil erosion including sheets and rills. Along with affecting soil loss, these activities also have an impact on on-site agricultural productivity and increase off-site sediment yields adjacent to the watershed outlet. On the other hand, the actual trends of soil losses and sediment yields have not yet been quantified apart from their importance for the hydroelectric dams in the basin and overall conservation measure suggestions based on soil loss severity.

This study aimed to quantify the impacts of spatiotemporal LULC dynamics on soil loss across agroecologies

and slope categories from 1985 to 2021 using GIS and RUSLE model in Zoa watershed. The specific objectives of this study were to: (1) quantify the impacts of spatiotemporal LULC changes on soil loss and determine soil loss variations across agroecologies and slopes, (2) determine the severity level of erosion in the sub-watershed and (3) evaluate temporal trends of sediment yields at the watershed outlet. The current study contributed to prioritizing soil erosion hotspot areas, which is vital for proper land use planning, conservation measures, policy development, and decision-making processes, thereby reducing soil losses in the watershed in turn averting sedimentation in the reservoirs of hydroelectric dams.

Materials and methods

Study area

Zoa watershed is situated in the Dawuro zone of southwest Ethiopia with a total area of 59,901.80 ha within the Omo-Gibe basin. Geographically, it lies between 7°3'00''–7°15'00''E and 37°2'00''E–37°23'00''E with an altitude extending from 914 to 3011 m above sea level (Fig. 1). It stretches the districts of Maraka, Gena, Loma Bossa, Zaba Gazo, and Tarcha Zuria of the Dawuro zone in the southwest regional state.

Geologically, the watershed is dominated by the middle basalt flows (33.83%) including primarily basalts with

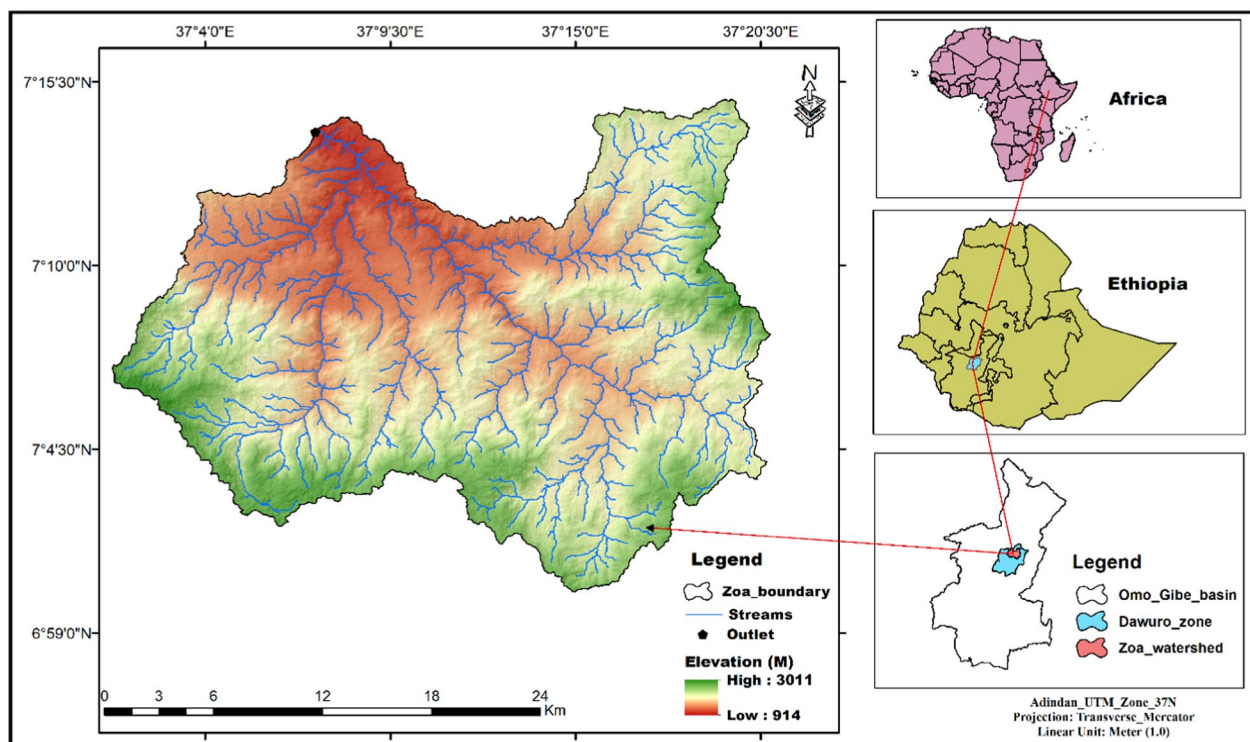


Fig. 1 Location of Zoa watershed in southwest Ethiopia. The watershed is situated in the northwestern part of the Dawuro zone within the Omo-Gibe basin

rare intercalation of trachyte, and trachyte flows (27.85%) which embrace mainly trachyte intercalated with minor ignimbrite and rare basalt. The southeastern margin, the central and southwestern parts of the watershed are under these types which comprised the major formations of the Cenozoic era in the upper tertiary period. The remaining northwestern and eastern parts of the watershed are subjugated by lower trachyte (20.34%) and lower basalt (17.34%). The lower trachyte flows contain rare pyroclastic materials and coal beds at places, while lower basalt flows comprise rare basaltic pyroclastic ingredients. They both are included in the lower tertiary period during the Cenozoic era. However, the small parts of the southwestern margin are covered by upper trachyte flows (0.64%) which comprised the formation of the upper tertiary period.

Based on the Digital Elevation Model (30 × 30 m resolution) inquiry, the watershed comprises three agroecologies (*Kola*, *Woinadega*, *Dega*) according to MOA (1998) Ethiopian traditional classes. *Kola* (lowland) covered 28.43% of the watershed and has an altitude extending from 914 to 1500 m above sea level. *Woinadega* (midland) has an altitude extending between 1500 and 2300 m above sea level and accounted for 63.91% of the watershed. About 7.65% of the watershed fell under *Dega* (highland) with an altitude of greater than 2300 m above sea level. The watershed has various terrain types including a flat surface, rugged landscape, and steep slope inclinations. This wide-ranging nature of the landscape is susceptible to many types of soil erosion from diverse land uses and slope terrains (Gitima et al. 2022). According to FAO (2006) slope classes in rises of percent, the slope of the watershed falls under gently sloping (0–5°), sloping (5–10°), and strongly sloping (10–15°) which accounts for 8.85%, 20.9% and 21.5% of the area, respectively. The remaining land area falls under moderately steep (15–30°), steep (30–60°), and very steep (>60°), with shares for 36.58%, 12.02%, and 0.08%, respectively.

The mean annual rainfall of the watershed ranges from 1201 to 1800 mm. The rainfall varies in the temporal season and has a bimodal pattern denoted by a short time of year in the spring season (March–May) and a prolonged time of year from June to September with a highest in August. The mean yearly minimum and maximum temperatures of the watershed extend from 14.65 °C to 16.12 °C and 26.4 °C to 29.3 °C, respectively (Gitima et al. 2021, 2022).

The majority of inhabitants in the Zoa watershed (91%) are farmers and rely on mixed agriculture as a source of income (Gebre et al. 2019). Despite the watershed’s great potential for agriculture, farmers typically use traditional farming techniques (oxen-plow and hoe farming cultures are practiced), which results in very low yields. The lifestyles of farmers are also relatively stagnant because agriculture is primarily rain-fed and market access is limited (Gitima et al. 2021). Land use classifications are decisive to quantify soil loss from the watershed. Accordingly, farmland, grassland, forestland, shrubland, and bareland are among the five major LULC classifications found in the research site. As indicated in Table 1, the descriptions of major LULC classes were identified in the study area.

Data sets

Three sets of longitudinal time series satellite images, namely: Landsat TM (1985), Landsat ETM+ (2000), and Landsat 8 OLI-TIRS (2021), were obtained from the USGS official website (<https://earthexplorer.usgs.gov/>) and used to produce LULC output maps and compute *P* and *C*-factors in the RUSLE model. We used a gap-filling method to reduce data inconsistencies and gaps in cloudy locations (where only a few clear-sky images per year are accessible in the study field during the dry season) as used by Gitima et al. (2022). To improve the accuracy of land use type classifications, all images of data sets were acquired from December to February 2021 with the minimum percentage of cloud cover. A random

Table 1 Identified major LULC classes in the Zoa watershed of the southwest regional state

Series no.	LULC classes name	Description
1	Farmland	The agricultural land of households including the strewn rural communities intimately allied to them. Because it was tough to differentiate strewn rural settlements as a distinct LULC class in areas with strewn cultivated areas, they were classified as single (Sisay et al. 2021)
2	Grassland	The watershed covered by grass temporarily is frequently cast off and fed for animal grazing (Belay and Mengistu 2019; Aneseeyee et al. 2020; Gitima et al. 2022)
3	Forest	The watershed is covered with dense trees including both plantation and natural trees, with an area that exceeds 0.5 ha (Sisay et al. 2021)
4	Shrubland	Sparsely spread scrubland trees and grasses interspersed with bushes cover the area (Degife et al. 2019; Aneseeyee et al. 2020)
5	Bareland	Areas with limited trees and a rocky landscape along the floodplains of local river valleys, on steep hillsides, and moderate slopes (Ogato et al. 2021)

sampling technique was employed to acquire an adequate number of training points, with a minimum sample size of 20 to 100 for each category of land use (Chen and Stow 2002). Reference points were used to perform accuracy assessments. Accordingly, basic field data from 294 current ground control truth sites in the study area were collected using GPS to determine the actual LULC classes. In addition, secondary data from the Ethiopian Geospatial Information Agency (EGIA) were obtained, such as a topographic map (scale 1:50,000) of the study area, to discern the geo-referencing operation for LULC class verifications and training sites, as well as to verify the quality of 1985 satellite images. Secondary data, including the Shuttle Radar Topography Mission-Digital Elevation Model, or SRTM-DEM (30 m resolution), was obtained in compressed files from the USGS official website (<https://earthexplorer.usgs.gov/>) to delineate the watershed and calculate slope and length factors. Furthermore, we obtained soil data from the Ethiopian MoWR (Ministry of Water Resources), such as a digital soil map (1:250,000 scale) premised on the FAO-UNESCO-ISRIC classification system for soils of the watershed, that was used to produce a *K*-factor map of the study area. Rainfall data in the form of stations and grid rainfall were acquired from Ethiopia's National Meteorological Agency (NMA) to compute the erosivity or *R*-factor of the study location.

Data analysis

Land cover analysis

The pre-processing approach in this work included geometric rectification, bad line spotting, image filtering, radiative calibration, and topographic adjustment (Tewabe and Fentahun 2020). To reduce sensor distortion, haze, remedial data loss, and missing lines caused by the solar situation and satellite calibration was performed (Aneseyee et al. 2020; Gitima et al. 2022). As a result, every Landsat image from the watershed was projected to the World Geodetic System (WGS_84_UTM Zone_37N) and geometrically adjusted with ground control points. Before enhancing image quality, atmospheric adjustments such as haze removal were undertaken. Furthermore, raw DN (digital number) measurements were translated into reflectance values for radiometric correction. Using the Earth Resource Data Analysis System (ERDAS) IMAGINE 2014 software, all-time series satellite pictures were removed or subset to encompass only the watershed territory. Thus, the maximum likelihood classifier for supervised classification was used in the present study, which assigned each pixel to the class with the highest probability (Sisay et al. 2021; Gitima et al. 2022).

An accuracy assessment was carried out based on the percentage of user and producer accuracy of the classified LULC classes by using the error matrix to verify

classified output maps for the referenced years. To analyze producer accuracy and overall accuracy as part of the entire accuracy assessment, the Kappa coefficient was employed (Sisay et al. 2021). Hence, the Kappa coefficient was calculated as follows (Eq. 1):

$$K_{\text{hat}} = \frac{N \sum_{i=1}^r X_{ii} - \sum_{i=1}^r (X_{i+} \times X_{+i})}{N^2 - \sum_{i=1}^r (X_{i+} \times X_{+i})}, \tag{1}$$

where K_{hat} refers to the Kappa coefficient, N refers to the total number of values, $N \sum_{i=1}^r X_{ii}$ refers to observed accuracy and $\sum_{i=1}^r (X_{i+} \times X_{+i})$ refers to chance accuracy.

Change detection was employed to identify the magnitude of alterations that take place over time and to classify changes in distinct LULC classes as then suitable judgments may be taken (Belete et al. 2020; Berihun et al. 2019; Gitima et al. 2022). As a result, the study area performed LULC change detection analysis during three distinct periods (1985–2000, 2000–2021, and 1985–2021). Minta et al. (2018) calculated the proportions of changes across time scales with percent and rate changes of different LULC classes using the following Eq. (2) and Eq. (3):

$$R\Delta(\%) = \left(\frac{X_2 - X_1}{X_1} \right) \times 100, \tag{2}$$

$$\text{Rate of change (ha /year)} = \left(\frac{X - X_1}{Y} \right), \tag{3}$$

where $R\Delta$ (%) represents the change of one type of LULC in percentage between the initial period (X_1) and the subsequent period (X_2) of a LULC class in hectares and Y denotes the time interval between X_1 and X_2 in a study year.

Soil loss estimation

The RUSLE is a universal model to estimate the rill and interrill soil erosion (Yesuph and Dagnew 2019; Kuli-mushi et al. 2021a, b), and to prioritize soil erosion risk areas (Tessema et al. 2020). According to Renard et al. (1997), the RUSLE model quantifies soil loss by comprising erosivity, soil erodibility, topographic factors, cover management, and conservation practices into consideration (Fig. 2; Eq. 4). Therefore, in this study, we used the RUSLE model to quantify soil loss adapted to Ethiopian situations by Hurni (1985). The RUSLE soil loss computation model Eq. (4) is given below:

$$A = R \times K \times LS \times C \times P, \tag{4}$$

where A =soil loss ($t \text{ ha}^{-1} \text{ year}^{-1}$), R =rainfall erosivity factor ($\text{MJ mm ha}^{-1} \text{ h}^{-1} \text{ year}^{-1}$), K =soil erodibility factor ($t \text{ ha}^{-1} \text{ MJ}^{-1} \text{ mm}^{-1}$), LS =slope-length and slope steepness factor (dimensionless), C =land management factor

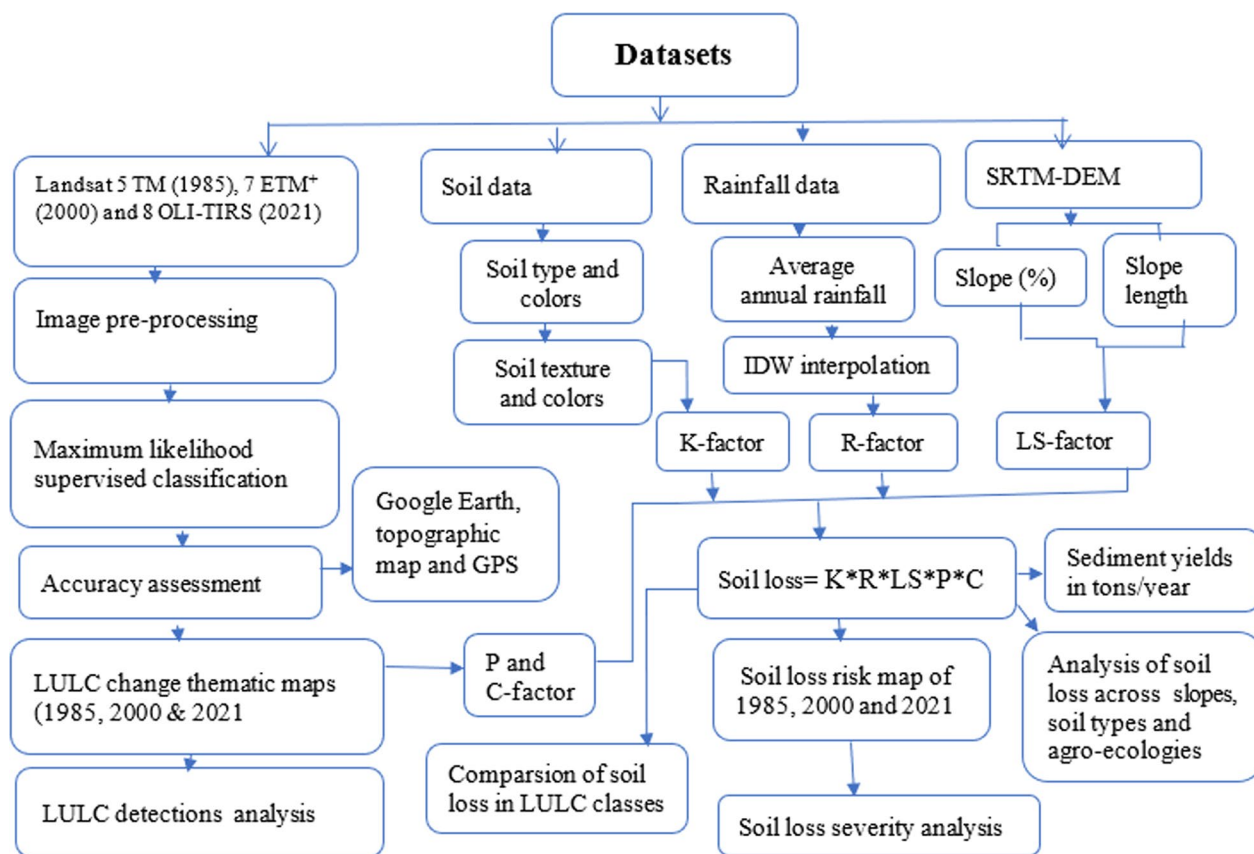


Fig. 2 Methodological flowchart of RUSLE model to compute soil loss and sediment yield

(dimensionless, ranges from zero to one), and P is the erosion support practice or conservation factor (dimensionless, ranges from zero to one). Each RUSLE factor raster layer was resampled to a grid of 30×30 m cell size resolution using a consistent coordinate system to estimate and map the temporal and spatial distribution of soil loss in the watershed. The layers were then multiplied pixel by pixel using Eq. (4) in the spatial analyst tools in the ArcGIS 10.8 environment (map algebra, raster calculator).

Rainfall erosivity (R) factor Rainfall erosivity is a multifaceted process in which the amount, intensity, energy, duration, pattern, and size of raindrops of rainfall and associated runoff exert influence on soil erosion (Farhan et al. 2013; Belayneh et al. 2019; Kulimushi et al. 2021a, b). However, it is difficult to apply equations directly in data-poor areas like Ethiopia. Instead, it was modified in the real situations of Ethiopia by Hurni (1985) to be applied using easily available mean annual rainfall data. The spatial regression equation is calculated using Eq. (5):

$$R = -8.12 + 0.562Z, \tag{5}$$

where R is rainfall erosivity ($\text{MJ mm ha}^{-1} \text{ year}^{-1}$) and Z is mean yearly rainfall (mm).

Hence, to compute the R factor, rainfall data of the study area were obtained from the Ethiopian metrological agency situated within and neighbors' stations. Accordingly, the strewn set of point rainfall data was interpolated by using Inversed Distance Weighting (IDW) toolset in ArcGIS 10.8 software to generate rainfall erosivity (Fig. 2) because the IDW method is the main eminent deterministic and it has been applied to altering spatial and transient scales due to its forthright feature (Ly et al. 2013).

K-factor or soil erodibility Soil erodibility is the manifestation of the inherent resistance of soil particles to the detaching and transporting power of rainfall (Wischmeier and Smith 1978). In this study, we applied the value of the K -factor based on the soil type and their associated colors, textures, and properties, which are indicators of soil vulnerability to erosion in the highlands of Ethiopia (Hurni 1985), and this approach was successfully used

by other studies (Molla and Sisheber 2017; Kidane et al. 2019; Aneseyee et al. 2020; Bekele and Gemi 2020). FAO standard classifications of soil type for our study area were extracted based on associated textural classes and respective colors due to rapid changes of LULC are indispensable (Zhang et al. 2013). For each soil type, *K*-value was dispensed and these values were transformed into a raster grid in the ArcGIS environment ensuing the standard technique (Table 2). A 1:250,000 scale map of the soil was used within the ArcGIS environment to determine *K*-values for each soil type.

Slope length and steepness (*LS*) factor The slope length (*L*) and steepness (*S*) factor replicate the effect of terrain and topography on soil attrition (Chang et al. 2016). The rise in slope length and slope inclines can result in a more overland flow swiftness and higher corrosion of erosion (Yahya et al. 2013). The steepness and length of the slope enhance the rate of noticeably water-induced soil erosion (Gashaw et al. 2018), through a greater accumulation of runoff (Wischmeier and Smith 1978). *LS*-factor was calculated in ArcGIS raster calculator spatial analyst tool using the map algebra expression in Eq. (6) proposed by Wischmeier and Smith (1978):

$$LS = \left(\frac{\text{Flow accumulation} \times \text{cell size}}{22.13} \right)^{0.4} \times \left(\frac{\text{Sin(Slope)}}{0.0896} \right)^{1.3} \tag{6}$$

where flow accumulation is a raster-based total accumulated flow in each cell weight for entire cells that flow into each downslope cell which is derived from DEM (30 m resolution) after processing fill and flow direction in ArcGIS, and cell size is the size grid cell derived from DEM.

Erosion management (support) practice (*P*-factor) The erosion control practice factor (*P*-factor) is the ratio of soil loss with a specific support practice to the consistent loss with upslope and downslope cultivation (Wischmeier and Smith 1978). During field inspections, we noticed poorly conceived physical land management practices, some of

which had collapsed owing to poor maintenance. It is difficult to determine *P*-values due to a lack of long-term conservation measures and inconsistencies in the application of conservation practices in complex rugged terrain in the watershed. Due to these reasons, we applied an alternative estimating process using the combination of LULC types and slope classes to compute *P*-factor output maps. Therefore, we adapted the corresponding *P*-values in each LULC and slope class as suggested by previous studies in Ethiopia (Wischmeier and Smith 1978; Hurni 1985; Gelagay and Minale 2016; Kidane et al. 2019; Yesuph and Dagnew 2019; Tessema et al. 2020) and that comprises two categories of land uses including farmland with corresponding slope inclinations and other land use classes (Table 3).

Land cover and management (*C*-factor) The *C*-factor indicates the proportion of soil loss from the land of a particular vegetation cover to the consistent soil loss from ceaseless fallow land (Wischmeier and Smith 1978). To determine the *C*-factor output maps, the three periods of LULC maps in raster form were converted to a polygon and consistent *C*-values were assigned to each LULC type preserved cover values (Table 4) as used in various parts of the country (Hurni 1985; Amsalu and Mengaw 2014; Gelagay and Minale 2016). Finally, using the spatial analyst tool in the ArcGIS environment, LULC vector maps were converted to *C*-factor maps in a raster format to adjust final RUSLE calculations.

Table 3 Conservation practices value (*P*-value) of Zoa watershed

Land use	Slope category (%)	<i>P</i> factors
Cultivated land	0–5	0.10
	5–10	0.12
	10–20	0.14
	20–30	0.19
	30–50	0.25
	50–100	0.33
Other land uses	All	1

Table 2 Identified soil types, colors, and erodibility values based on FAO standards of Zoa watershed

Soil types	Textural classes	Soil color	<i>K</i> -factor	Area in ha
Dystric nitisols	Clay loam	Red	0.25	38,589.23
Orthic acrisols	Loamy sand	Yellow	0.33	13,846.4
Eutric cambisols	Sandy loam	Very dark gray	0.35	5078.38
Dystric fluvisols	Coarse sand to clay	Yellow	0.30	1360.7
Dystric gleysols	Sandy clay loam to clay	Brown	0.31	1027.08

Table 4 Land use types and their corresponding C-values of Zoa watershed

Land use types	C-values	Sources
Farmland	0.15	Hurni (1985), Adugna et al. (2015), Yesuph and Dagne (2019) and Belay and Mengistu (2021)
Bareland	1	Hurni (1985) and Renard et al. (1997)
Forest	0.01	Molla and Sisheber (2017) and Yesuph and Dagne (2019)
Grassland	0.11	Kidane et al. (2019)
Bushland	0.05	Molla and Sisheber (2017)

Table 5 The overall accuracy assessment of LULC types for 1985, 2000 and 2021 in the Zoa watershed

LULC types	1985		2000		2021	
	User accuracy	Producer accuracy	User accuracy	Producer accuracy	User accuracy	Producer accuracy
Bareland	92.3	80.0	82.61	82.6	84.21	78.05
Farmland	87.3	91.2	93.41	94.4	93.6	96.7
Forest	91.8	90.33	92.54	93.9	91.9	87.18
Grassland	81.4	77.8	88.89	84.2	87.09	81.8
Shrubland	87.01	89.3	90.74	90.74	87.3	90
Overall accuracy	87.55	87.55	91.14	91.14	89.79	89.79
Kappa statistics	83.72	83.72	88.39	88.39	86.07	86.07

Sediment yield valuation

It is imperative to compute sediment yields from a catchment to reduce the deposition rate at the watershed outlet. The RUSLE model does not compute the amount of sediment yield from a catchment outlet. Sediment yield is premeditated from annual soil loss by multiplying it with the sediment delivery ratio as proposed by Dinka (2020). According to Bekele and Gemi (2020), the sediment delivery ratio (SDR) depicts the relationship between sediment yield at a certain stream cross-section and entire erosion from the watershed upstream of the measuring station. According to Bekele and Gemi (2020), the sediment yield at the watershed outlet was computed using the empirical formula as Eq. (7):

$$SDR = A^{-0.2}, \tag{7}$$

where SDR refers to the sediment delivery ratio and A refers to an area of the watershed. The value of SDR for an area is found to be affected by catchment physiography, sediment sources, transport system, the texture of eroded material, land cover, etc. (Dinka 2020). The SDR is the ratio of sediment transported to the outlet through the watershed, including both channel and overland sediment (Bekele and Gemi 2020). Therefore,

according to them, the sediment yield was commonly computed by the following empirical formula (Eq. 8):

$$Sy = E \times \left(\frac{1}{A^{0.2}} \right), \tag{8}$$

where Sy=sediment yield (ton) at the watershed outlet; E=total erosion (t); and A=area of the watershed in ha.

Validation approaches of the RUSLE model

An integrated RUSLE, GIS, and remote sensing method were found valuable tools for quantifying soil erosion, variability, and sub-watershed prioritization, particularly in data-poor countries like Ethiopia (Belayneh et al. 2019). Google Earth data sets and regular field observations (ground control sites) were used to validate the RUSLE parameters such as C and P-factors. Due to the lack of previous case studies in our study area, we compared our quantified soil losses to similar studies conducted in various parts of the Ethiopian highlands (Amsalu and Megaw 2014; Gemechu 2016; Haregeweyn et al. 2017; Moges and Bhat 2017; Yiferu et al. 2018; Chimdessa et al. 2018; Gashaw et al. 2020; Girmay et al. 2020; Tessema et al. 2020; Woldemariam and Harka 2020).

Results

Spatiotemporal LULC dynamics in the watershed

The overall accuracies of LULC classified images were ascertained to be 87.55% in 1985, 91.14% in 2000, and 89.79% in 2021 (Table 5). The overall Kappa statistics for output maps show that the LULC images correctly classified for 1985, 2000, and 2021 were observed to be 83.72, 88.39, and 86.07, respectively.

Farmland and shrubland comprised the majority of the watershed in 1985, next by grassland (17.15%), woodlandforest (10.19%), and bareland (1.7%). Farmland, shrubland, and forest area's respective proportions in 2000 were 51.46%, 23.98%, and 11.97%. Bareland (6.59%) and grassland (6%) comprised the remaining sections of the watershed. Farmland (71.12%), shrubland (12.6%), and forest (7.3%) were identified in spatial heterogeneity in the year 2021. During the same year, the watershed's remarkable amounts were grassland (2.09%) and bareland (6.89%). The patterns of LULC dynamics differ substantially between land use types throughout three reference study periods. During the study periods (1985–2021), shrubland, grassland, and forest had a diminishing with rates of -1.89% , -2.37% , and -0.77% year⁻¹, respectively as a result of the watershed-induced spread of deforestation, agricultural acreage, and population

increase (Fig. 3). However, since a significant portion of shrubland and grassland was turned into farmland at a rate of 448.85 ha (1.05%) and 250.74 ha (0.58%) each annum, respectively, farmland noted the rising trends from 29.09% in 1985 to 71.12% in 2021 (Fig. 3).

Parameterization of the RUSLE model

R-factor, LS-factor and K-factor

Using Eq. (5), the range of the rainfall erosivity (*R-factor*) is found to be between 730.965 and 945.689 MJ mm ha⁻¹ year⁻¹. The eastern and western margins of the watershed had the highest *R-factor*, indicating extreme erosivity and having contributed to the maximum soil loss, while the southeastern and central portions of our research location had the lowest *R-factor*, indicating the lowest erosivity and soil loss of the area (Fig. 4a).

The *LS* factors of the Zoa watershed range from 0 in gentle terrain to 229.798 in very high hillslopes, as shown in Fig. 4b. As the slope inclinations rise, the *LS* values rise, indicating a probable increase in soil loss due to erosion. The *K*-value for certain soil classes was calculated using soil texture classifications and soil colors based on FAO standards. The *K-factor* of the soils in the watershed has five typical erodibility values that varied from 0.25 to 0.35 depending on the color of the soil (Fig. 4c). Accordingly,

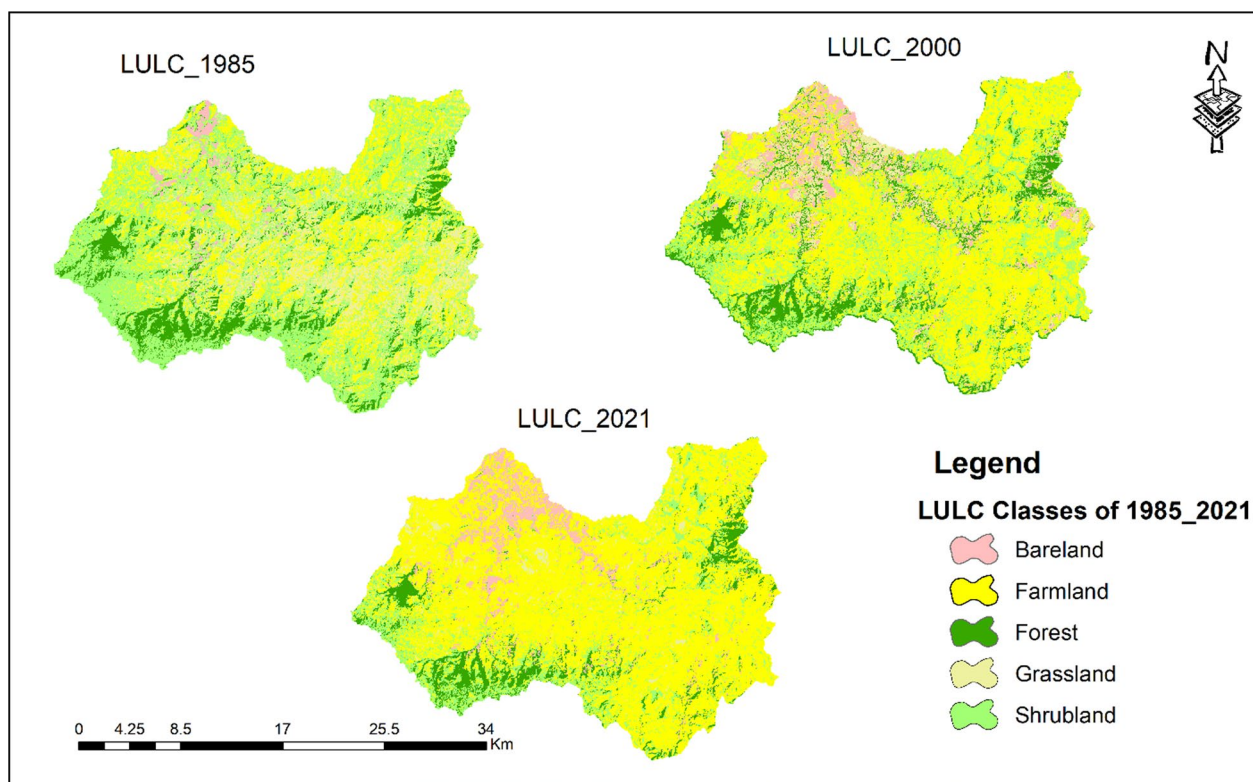


Fig. 3 Classified LULC maps for 1985, 2000, and 2021 in the Zoa watershed

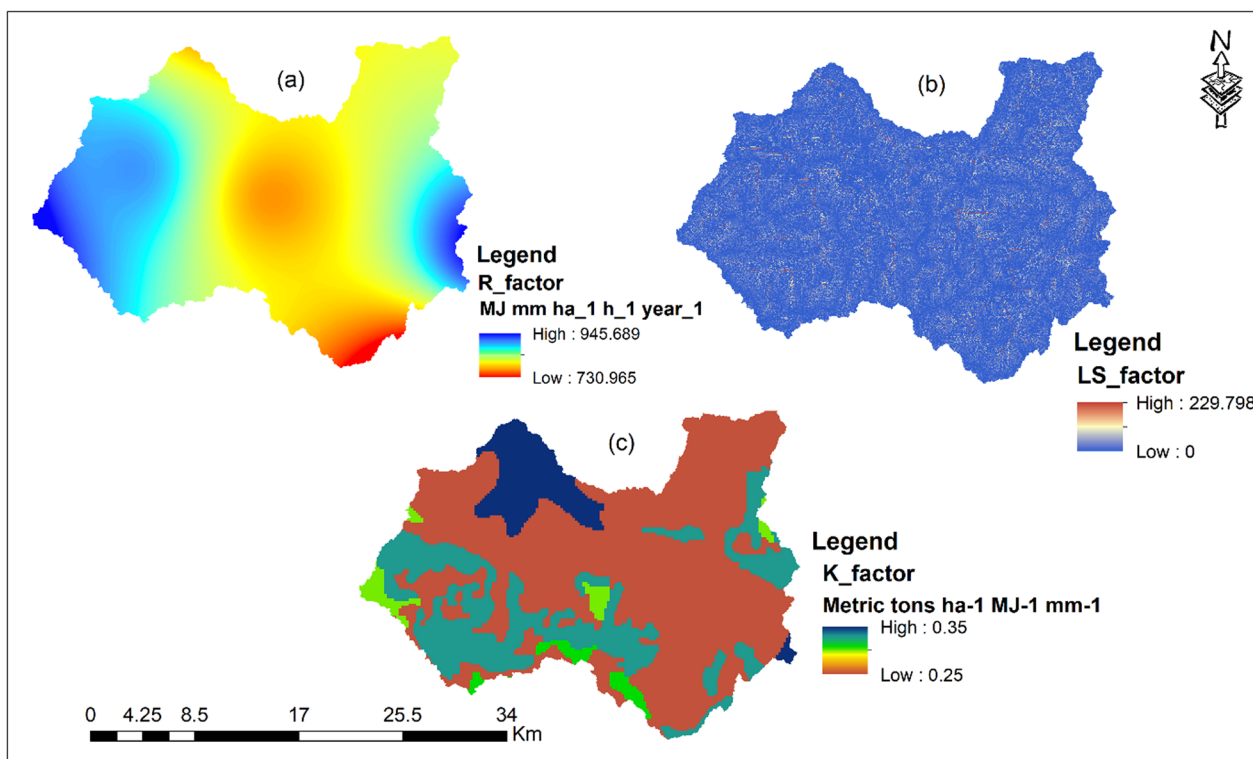


Fig. 4 Map of Zoa watershed showing *R*-factor (a), *LS*-factor (b), and *K*-factor (c)

Eutric cambisols, orthic acrisols (23.12%), and dystric gleysols (1.71%) have the highest valued *K*-factor of 0.35, 0.33, and 0.31 in the watershed, respectively. However, dystric nitisols and fluvisols were observed the lower than further with the *K*-values of 0.25 and 0.30 accounted 64.42% and 2.27%, respectively. In contrast, a higher *K*-value indicates more vulnerability to soil erosion, while a lower *K*-value designates lesser vulnerability to erosion (Tessema et al. 2020; Bekele and Gemi 2020).

C-factor and P-factor

Soil erosion is most significantly impacted by LULC dynamics in the watershed. The *C*-values for the watershed were increased for each of the five LULC types, as shown in Fig. 6, from zero to one. The *C*-value tends to be zero, denoting appropriate management practices and accelerating lower soil losses, whereas the *C*-values tend to be one, denoting insufficient or no management practices and accelerating greater soil losses (Fig. 5). The lower *C*-values were found in forest (0.01) and shrubland (0.05), while the larger *C*-values were noted in grassland (0.11), farmland (0.15), and bareland (1) between 1985 and 2021, according to the pixel-based categorized maps of LULC classes (Fig. 5).

As shown in Fig. 6, farmland was categorized into six slope terrains, each of which was assigned a *P*-value, but all other land use classifications had only one *P*-value due to the importance of the slope gradients of the farmland in erosion conservation strategies (Fig. 6). Therefore, the lower the *P*-values, the more effective is the practices of protecting soil erosion. For instance, forest areas had a lower human interface than farmland, due to this they had the lowest *P*-values as compared with all land use types. In contrast, farmland with the steepest slope terrains had the highest *P*-value, whereas farmland with the gentlest slopes in the watershed had the lowest *P*-value (Fig. 6). This is because cultivation in marginal areas has increased to high gradients. As a result, a tolerance level of zero indicates a high level of support for behaviors that contribute to human-induced soil loss, whereas a tolerance level of 1 indicates a low level of support for those practices.

Spatiotemporal soil loss rate in Zoa watershed

Due to the watershed’s rugged topography and LULC alterations, the average yearly soil loss rate varies in both space and time. The analysis indicates that the watershed’s annual soil loss varied from 0 on flat surfaces to 113.21 t ha⁻¹ year⁻¹ on extremely steep terrain, 0 to

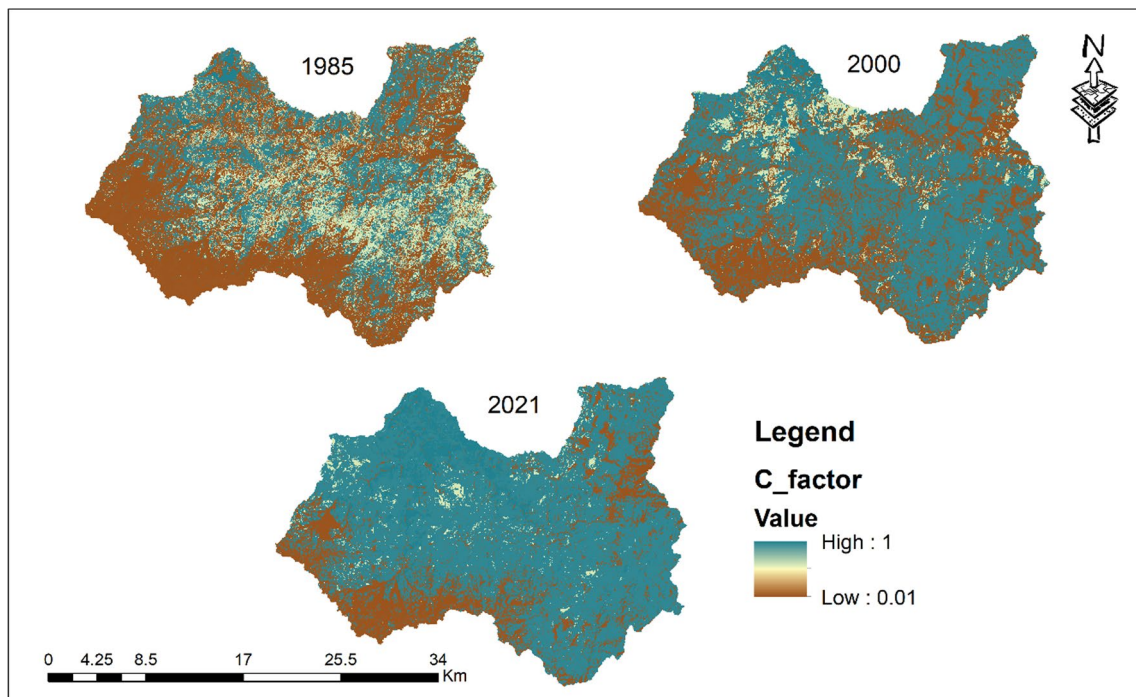


Fig. 5 Spatial distributions of the C-factor map between 1985 and 2021 of Zoa watershed

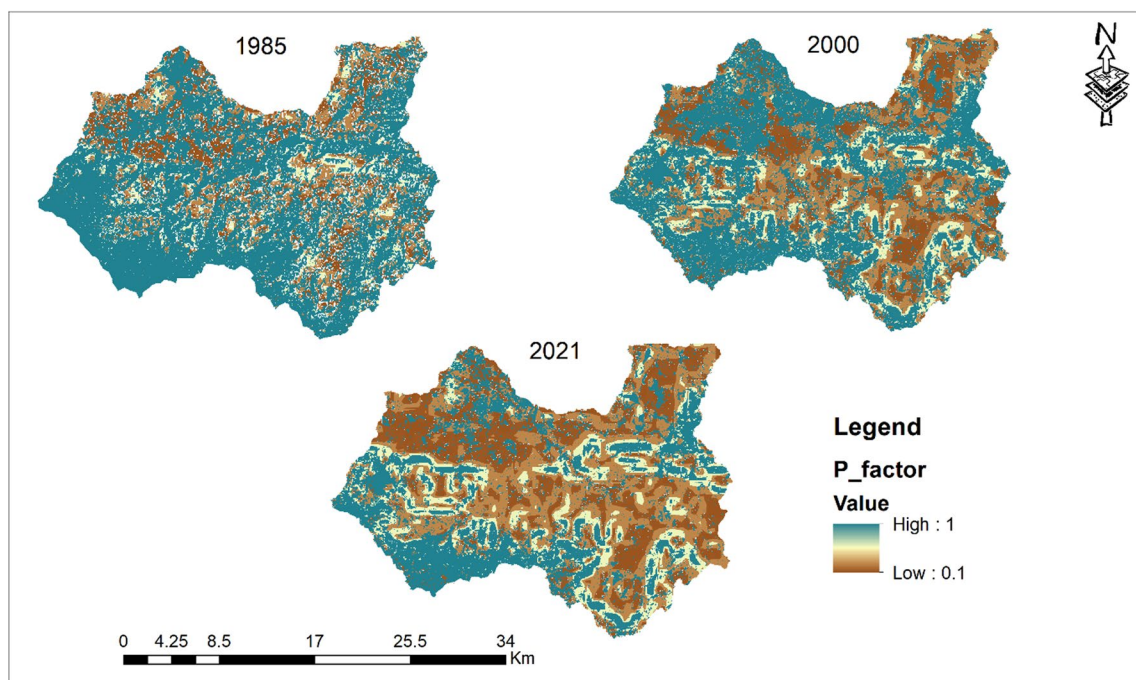


Fig. 6 Spatial distributions of the P-factor map between 1985 and 2021 of Zoa watershed

163.16 t ha⁻¹ year⁻¹ and 0 to 194.58 t ha⁻¹ year⁻¹ with an average yearly soil loss of 21.07 t ha⁻¹ year⁻¹ in 1985, 29.35 t ha⁻¹ year⁻¹ in 2000, and 40.93 t ha⁻¹ year⁻¹ in

2021. The gross soil losses of the watershed were found to be 1.26 million ton year⁻¹ in 1985, 1.75 million ton year⁻¹ in 2000 and 2.45 million ton year⁻¹ in 2021.

The average soil loss ratings, which ranged from less than 5 t ha⁻¹ year⁻¹ to more than 50 t ha⁻¹ year⁻¹, were adopted by Haregeweyn et al. (2017), Zerihun et al. (2018), and Gashaw et al. (2020). The soil loss rates were divided into five categories premised on their severity levels: 0–5 t ha⁻¹ year⁻¹, 5–11 t ha⁻¹ year⁻¹, 11–30 t ha⁻¹ year⁻¹, 30–50 t ha⁻¹ year⁻¹, and > 50 t ha⁻¹ year⁻¹, which pertained to the severity levels of very slight, slight, moderate, severe, and very severe (Fig. 7).

As a result, the Zoa watershed’s spatial soil loss rates varied greatly and were ascribed to various changes in topography, soil types, and land use. Figure 7 illustrates how the watershed’s northwest and eastern portions had above-acceptable soil loss, which was considerably expanded into the study site’s middle and southern regions.

The spatiotemporal distributions and patterns of soil loss in the watershed varied from 1985 to 2021, as shown in Table 5. According to the findings on soil severity, the dominant 39,547.91 ha (66.02%) areas of the watershed in 1985 produced a soil loss rate of 0–5 t ha⁻¹ year⁻¹. The watershed experienced moderate soil loss and severe soil loss, which accounted for 10,394.15 ha (17.35%) and 7385.82 ha (12.33%) of the watershed area, respectively. The watershed also encountered very severe soil loss, which comprised

1336.93 ha (2.23%) and 1236.99 ha (2.07%). In 2000, proportions of the watershed generated a soil loss rate of very slight (0–5 t ha⁻¹ year⁻¹), slight (5–11 t ha⁻¹ year⁻¹), moderate (11–30 t ha⁻¹ year⁻¹), severe (30–50 t ha⁻¹ year⁻¹) and very severe (> 50 t ha⁻¹ year⁻¹) comprised 38,710.10 ha (64.62%), 9382.03 ha (15.66%), 6798.10 ha (11.35%), 1822.94 ha (3.04%), and 3188.63 ha (5.32%), respectively. In 2021, the watershed produced moderate soil loss, severe soil loss and very severe soil loss were considered 14,259.50 ha (23.80%), 3553.40 ha (5.93%), and 6194.08 ha (10.34%), respectively. An analysis of pixel-based soil loss risk maps revealed that between the years 1985 and 2021, around –40.77% of the watershed was characterized by a soil loss rate of 0–5 t ha⁻¹ year⁻¹ (Table 6). Moreover, the watershed experienced soil loss in the range of 5–11 t ha⁻¹ year⁻¹, 11–30 t ha⁻¹ year⁻¹, 30–50 t ha⁻¹ year⁻¹, and > 50 t ha⁻¹ year⁻¹ were the soil loss rates of 19.98%, 93.07%, 165.79%, and 400.74%, respectively, between 1985 and 2021. These show that during the studied periods, the quantity of mean annual soil loss increased. Farmland expands to steep slopes, improperly designed physical conservation methods, overgrazing, and shrinking forest resources all contributed to the rising trends in soil loss.

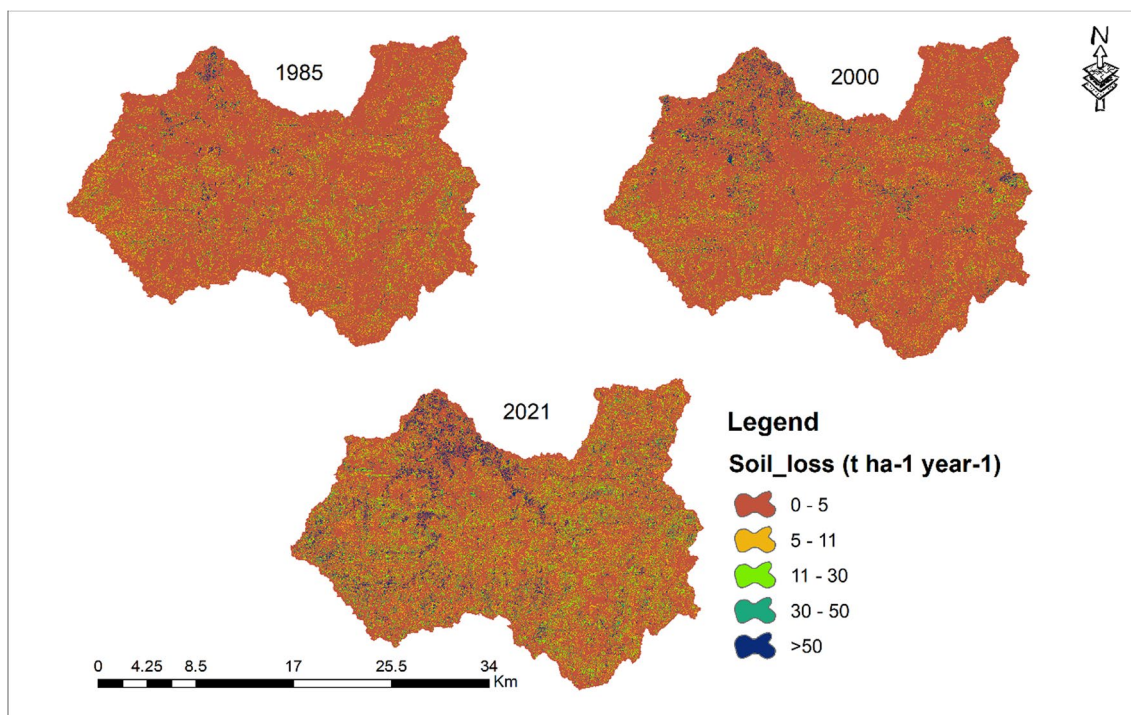


Fig. 7 Spatiotemporal annual soil loss risk map in 1985, 2000 and 2021 in the Zoa watershed

Table 6 Spatiotemporal area, trends and quantified each soil loss rate in the Zoa watershed during 1985–2021

Mean soil loss rate (t ha ⁻¹ year ⁻¹)	1985		2000		2021		1985–2000		2000–2021		1985–2021	
	Area (ha)	%	Area (ha)	%	Area (ha)	%	Area (ha)	%	Area (ha)	%	Area (ha)	%
0–5	39,547.91	66.02	38,710.10	64.62	23,424.19	39.10	– 837.81	– 2.12	– 15,285.91	– 39.49	– 16,123.72	– 40.77
5–11	10,394.15	17.35	9382.03	15.66	12,470.63	20.82	– 1012.11	– 9.74	3088.60	32.92	2076.48	19.98
11–30	7385.82	12.33	6798.10	11.35	14,259.50	23.80	– 587.72	– 7.96	7461.40	109.76	6873.68	93.07
30–50	1336.93	2.23	1822.94	3.04	3553.40	5.93	486.01	36.35	1730.46	94.93	2216.47	165.79
> 50	1236.99	2.07	3188.63	5.32	6194.08	10.34	1951.63	157.77	3005.45	94.26	4957.09	400.74
Total	59,901.8	100	59,901.8	100	59,901.8	100	–	–	–	–	–	–

Table 7 Spatiotemporal area of each land use type and their respective quantified mean yearly soil losses (t ha⁻¹ year⁻¹) in 1985, 2000 and 2021 of Zoa watershed

LULC types	1985			2000			2021		
	Area (ha)	%	Mean soil loss	Area (ha)	%	Mean soil loss	Area (ha)	%	Mean soil loss
Bareland	1017.10	1.70	31.73	3951.27	6.59	39.04	4128.69	6.89	35.52
Farmland	17,425.70	29.09	27.08	30,823.99	51.46	53.58	42,604.20	71.12	59.91
Forest	6104.03	10.19	4.50	7168.34	11.97	8.08	4372.21	7.30	6.61
Grassland	10,273.16	17.15	20.48	3593.93	6.00	17.15	1251.38	2.09	19.19
Shrubland	25,081.80	41.87	16.22	14,364.26	23.98	19.06	7545.32	12.60	24.00

Impacts of spatiotemporal LULC dynamics on soil loss

In the watershed, soil loss from erosion hazards varied widely in spatiotemporal LULC dynamics (Table 7). Due to the maximum severity of soil erosion rates from unprotected surfaces, the highest soil losses among LULC classes were quantified from bareland (31.73 t ha⁻¹ year⁻¹) and farmland (27.08 t ha⁻¹ year⁻¹) in 1985, which later increased to 35.52 t ha⁻¹ year⁻¹ and 59.91 t ha⁻¹ year⁻¹, respectively, in 2021. Additionally, there was excessively high soil loss in grassland and shrubland, with losses of 20.48 t ha⁻¹ year⁻¹ and 16.22 t ha⁻¹ year⁻¹, respectively, that later fluctuated to 19.19 t ha⁻¹ year⁻¹ and 24.0 t ha⁻¹ year⁻¹ in 2021 (Table 7). Due to the increase in livestock populations and agricultural expansion in the research area, these situations may be a result of the diminishing tendencies of grassland and shrubland areas.

Soil loss variation across agroecologies and slope gradients

We also extracted and identified three agroecological settings’ mean soil loss range from the entire soil erosion hazard maps to detect rigorous soil loss risk areas and propose better land management planning. The result specified that the lowland (*Kolla*) agroecology ascertained the prevalent mean soil loss, which

was anticipated to be 24.05 t ha⁻¹ year⁻¹ in 1985, 39.74 t ha⁻¹ year⁻¹ in 2000, and 57.55 t ha⁻¹ year⁻¹ in 2021 (Fig. 8a). This may be because lowland areas are primarily covered by bareland land use class, which increases the risk of soil erosion. The quantified mean annual soil loss of 16.16 t ha⁻¹ year⁻¹, 27.42 t ha⁻¹ year⁻¹, and 38.81 t ha⁻¹ year⁻¹ was generated from the midland (*Woinadega*) in the years 1985, 2000, and 2021, respectively. In contrast, the mean yearly soil loss of 10.09 t ha⁻¹ year⁻¹ in 1985, 22.21 t ha⁻¹ year⁻¹ in 2000, and 21.82 t ha⁻¹ year⁻¹ in 2021 produced from the highland (*Dega*) agroecology which is the lowest soil loss range, because the highland area in the study’s setting is primarily covered by forests.

The soil loss hazard output maps were extracted from the entire watershed in each study period conferring to the slope gradients, because slope gradients are the foremost factors to accelerate soil erosion in the study site due to rugged topography. The outcome showed that the risk of soil loss is rising with slope gradients. As shown in Fig. 8b, the lowest mean soil loss (8.16 t ha⁻¹ year⁻¹) was generated from flat (0–5) surfaces in 1985, which later rose to 30.47 t ha⁻¹ year⁻¹ in 2021. In contrast, the highest and most excruciating soil loss was engendered from steep (35.55–60.78 t ha⁻¹ year⁻¹) and very steep

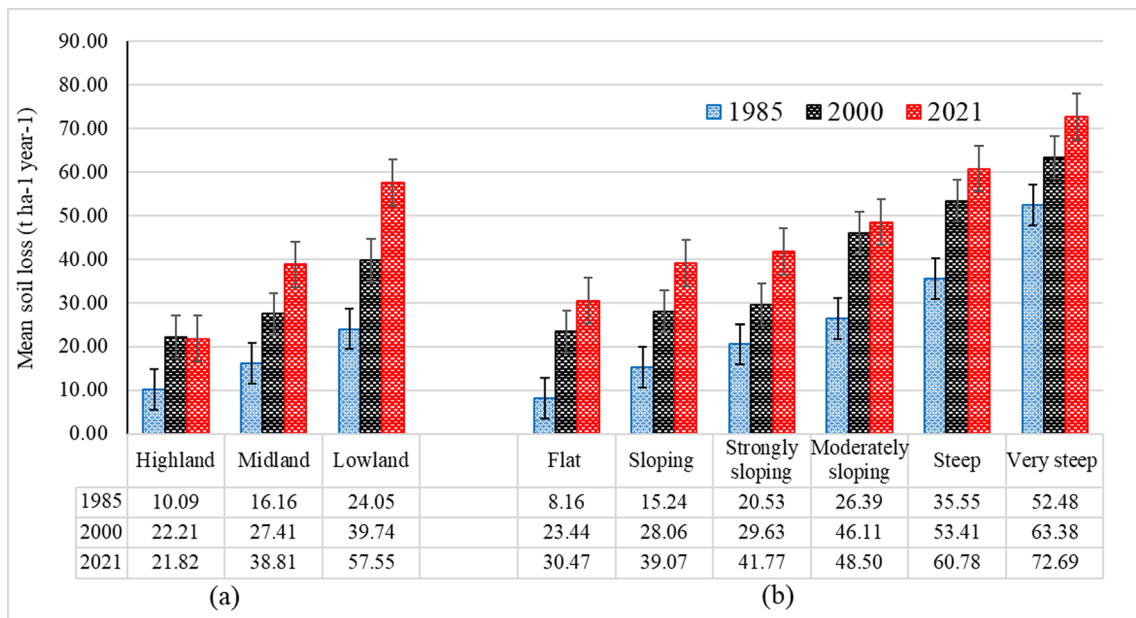


Fig. 8 Mean yearly soil losses under three agroecologies (a), and slope gradients (b) of three study periods (1985, 2000 and 2021) in all land use types of Zoa watershed. Flat = 0–5°; sloping = 5–10°; strongly sloping = 10–15°; moderately sloping = 15–30°; steep = 30–60°; very steep ≥ 60°

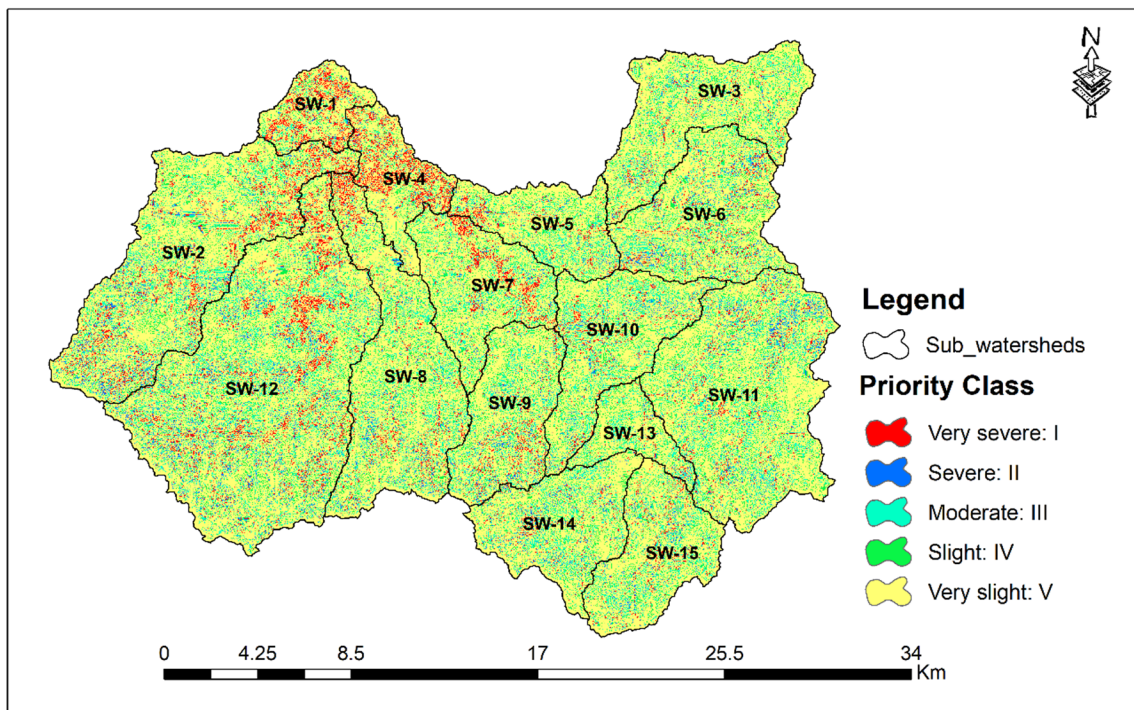


Fig. 9 Soil loss severity map at the sub-watershed level of 2021 in Zoa watershed

(52.48–72.69 t ha⁻¹ year⁻¹) slope gradients between the study period of 1985–2021. These suggest applying appropriate land management practices in the study site.

Soil loss severity analysis at the sub-watershed level

To execute the current and future effective conservation planning from the entire watershed, it is crucial to identify observed soil loss rate and fragility at the sub-watershed level. We used soil erosion risk maps for the year 2021 to identify severity groups for optimum land management practices. Among the 15 reflexive delineated sub-watersheds, the mean soil loss produced and categorized as very severe (> 50 t ha⁻¹ year⁻¹) was observed in SW-1 (84,886.18 ha, 4.31%), SW-2 (407,776.26 ha, 20.71%), SW-4 (93,766.59, 4.76%), SW-7 (153,571.69 ha, 7.8%) and SW-12 (618,749.04 ha, 31.42%) from the entire watershed (Fig. 9). This excessive soil loss may be related to the type of bareland, incompatible land management practices, and enormously high slope terrains. These sub-watersheds were consequently given a high priority to signify proper conservation planning. The conservation strategy, which includes area closure, building soil bunds, and planting trees and stone bunds, may reduce soil erosion hazards. The mean soil loss generated and classified as severe (30–50 t ha⁻¹ year⁻¹) was observed in SW-5 (70,118.31 ha, 3.56%) and SW-11 (216,295.56 ha, 11.0%), while the mean soil loss risk rate under moderate (11–30 t ha⁻¹ year⁻¹) was observed in SW-6 (46,098.18 ha, 2.34%), SW-8 (84,689.95, 4.30%), SW-9 (43,654.39 ha, 2.22%), SW-10 (42,341.96 ha, 2.15%) and SW-15 (32,998.89 ha, 1.68%). Henceforth, these sub-watersheds are required as the second and third

priority for soil erosion conservation strategies, respectively. Mechanical conservations such as check dams and terraces with appropriate designs could be recommended to reduce soil loss risks. The three sub-watersheds fell under a yearly soil loss range of slight (5–11 t ha⁻¹ year⁻¹) including SW-13 (9558.41 ha, 0.49%) SW-3 (36,935.83 ha, 1.88%), and SW-14 (27,562.31 ha, 1.40%) due to the minimum percent of forests (Fig. 9).

Sediment yields

We computed the sediment delivery at the watershed outlet using Eq. (8) throughout three research periods to assess the relationship between the gross soil loss from a watershed and the sediment delivery ratio. The pixel-based study revealed that in 1985, the watershed outlet produced sediment yields of 139,835.18 t year⁻¹ from soil losses of 1,262,130.93 t year⁻¹ (Fig. 10). In 2000 and 2021, the gross soil loss of 1,758,117.83 t year⁻¹ and 2,451,780.67 t year⁻¹ generated sediment yields for 194,787.01 t year⁻¹ and 271,639.95 t year⁻¹ at the watershed outlet in 2000 and 2021, respectively. The sediment yield tendencies at a watershed outlet grew at the maximum rate, from 39.3% in 1985 to 94.26% in 2021.

Discussion

Historical LULC change

From 1985 to 2021, the spatial and temporal magnitude of various LULC changes is illustrated (Fig. 3). Considerable LULC conversions have been observed at these times, with a notable LULC conversion index. Due to the increase in livestock, the spatial coverage of grassland exhibited a falling tendency over time of – 87.8% or – 2.37% year⁻¹. Similarly, forest area (– 28.4%, – 0.77%

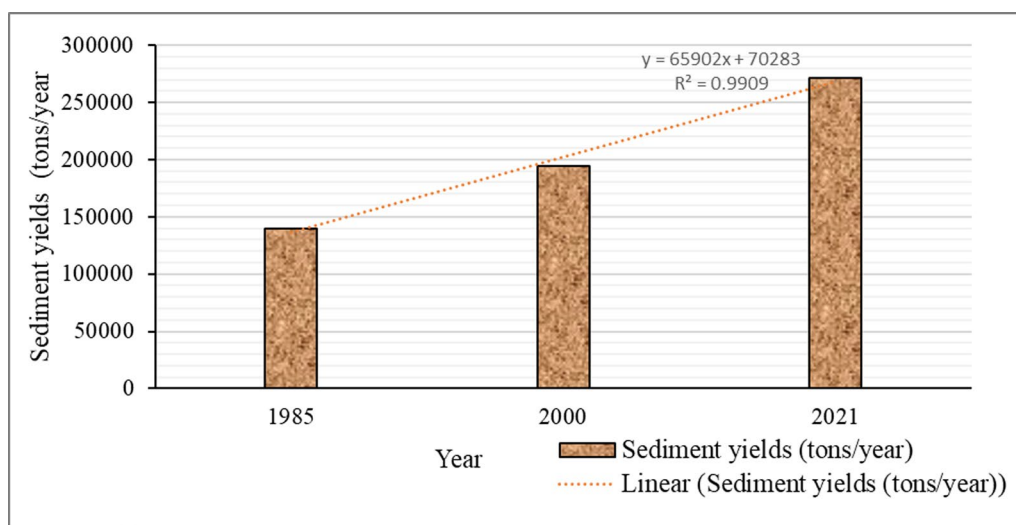


Fig. 10 Gross sediment yields of Zoa watershed in 1985, 2000 and 2021

year⁻¹) and shrubland (− 69.9%, − 1.89% year⁻¹) showed a decreasing trend, which is related to a rise in deforestation, farmland, and population growth between 1985 and 2021. These alterations were brought about by the continuous conversion of a substantial tract of forest (1112.20 ha) and shrubland (16,607.43 ha) into farmland. Previous research highlighted the dwindling trends of grassland, shrubland, and forest in various Ethiopian areas: Agidew and Singh (2017) in Teleyayen sub-watershed; Belay and Mengistu (2019) in the Upper Blue Nile basin; Betru et al. (2019) in the Assosa zone; Dibaba et al. (2020) in Finchaa Catchment; Ogato et al. (2021) in Huluka watershed and Tolessa et al. (2020) in Didessa sub-basin.

The maximum percentage of bareland increased due to the extension of overgrazing in the watershed's outlet area by 288.5%, or 7.8% per year, from 1985 to 2000 and 305.9%, or 8.27% per year, from 2000 to 2021. From the northwest to the south portion, it was somewhat extended. Although rain-fed agriculture is the primary source of subsistence, farmland also demonstrated expanding tendencies, rising by 76.89% between 1985 and 2000 and 144.5% or 3.9% year⁻¹ between 2000 and 2021 (Fig. 3). According to Potapov et al. (2022), the continent of Africa has observed the greatest net increase of agriculture worldwide, followed by Asia and South America. This expansion is reminiscent of sub-Saharan Africa in general (Bullock et al. 2021) and East Africa in particular since rising food demand is driving more agricultural output (Kulimushi et al. 2021a). Moreover, recent LULC change studies in various areas of the country have shown that cropland is expanding at the expense of shrubland and forestland (Gashaw et al. 2018; Minta et al. 2018; Belay and Mengistu 2019; Betru et al. 2019; Degife et al. 2019; Gessesse et al. 2019; Hailu et al. 2020; Ogato et al. 2021; Sisay et al. 2021).

Impact of LULC change on soil erosion and sediment yields

The RUSLE factors' findings demonstrated the watershed's significant erosional potential by revealing the effect of different erosion factors. Soil erosivity is hence determined by five different factors. The determination of each RUSLE factor on soil loss was interdependent. The range of the rainfall erosivity (*R*-factor) is found to be between 730.965 and 945.689 MJ mm ha⁻¹ year⁻¹ in our study area. The results showed that the eastern and western margins of the Zoa watershed had the highest *R*-factor, reflecting the greatest erosivity. Consistently, the spatial variations of the *R*-factor are not perfectly associated with rainfall erosivity in tropical regions (Kulimushi et al. 2021a; b). In comparison, the *R*-values of the

Zoa watershed are notably lower than the average value of global erosivity (2000 MJ mm ha⁻¹ year⁻¹) (Borrelli et al. 2017). Comparable findings have been reported in the Ethiopian highlands for the observed *R*-value range in the Zoa watershed (Amsalu and Mengaw 2014; Gelagy and Minale 2016; Haregeweyn et al. 2017). Kidane et al. (2019), Tessema et al. (2020), and Belay and Mengistu (2021) noticed that soil erosion is influenced by rainfall because erosivity determines soil loss.

The important determining element for the increase in soil erosion severity is the *LS* factor. Our study revealed that the *LS* factor varied from 0 to 229,798. This is due to the upsurge in kinetic energy of movements produced by slope disposition rises (Nehai and Guettouche 2020). These findings agreed with previous studies in the country (Amsalu and Mengaw 2014; Tadesse et al. 2017; Yiferu et al. 2018; Bekele et al. 2019; Gashaw et al. 2019; Yesuph and Dagneu 2019; Tessema et al. 2020; Bekele and Gemi 2020). Moreover, Renard et al. (1997) argued that the slope gradients determine the velocity of flow, while the slope length designates the detachment from where the derivation of the soil erosion to the sediments. The eutric cambisol type was found to have the greatest erodibility value out of the five different soil types. Previous studies reported similar results (Tessema et al. 2020; Bekele and Gemi 2020). Kulimushi et al. (2021a, b) found that cambisols are highly susceptible to soil erosion in tropical and subtropical regions, which are fragile, have low drainage capacities, and are subject to erosion.

The variation in soil erosion was consequently attributed to the *C*-factor, which varied as the LULC changed in space and time. While the other RUSLE variables remained constant, the variations of the temporal *C*-factor were noticed owing to LULC dynamics (Kulimushi et al. 2021a; b). Consequently, the mean yearly soil loss in the Zoa watershed increased from 21.07 t ha⁻¹ year⁻¹ in 1985 to 40.93 t ha⁻¹ year⁻¹ in 2021. The soil loss intensified as a result of the enormous amount of shrubland and forest that was turned into farmland throughout time. These findings were comparable to the range of global yearly soil losses (30 to 40 t ha⁻¹ year⁻¹) valuation (Pimental et al. 1995). It is analogous to that of soil loss from steep gradient areas of farmland for hilly watersheds in Poland of Europe (Kijowska-Strugała et al. 2018) and north Morocco of Africa (Amellah and Morabiti 2021). In comparison, soil losses in European countries such as Austria and Italy were four times lower than at our research location (Fenta et al. 2020). In other places of the world, however, scholars calculated far higher severe soil loss rates than those observed in this study. Similarly, the maximum soil losses were registered in many parts of Africa as compared with our study watershed. For

example, the results reported the average soil losses for an entire part of Rwanda, $250 \text{ t ha}^{-1} \text{ year}^{-1}$ (Karamage et al. 2016); Jijel Wilaya of Algeria, $286.4 \text{ t ha}^{-1} \text{ year}^{-1}$ (Nehai and Guettouche 2020); South-Kivu province of Democratic Republic of Congo, $138.2 \text{ t ha}^{-1} \text{ year}^{-1}$ (Kulimushi et al. 2021a; b) and Maradi Region of South-Central Niger, $472.4 \text{ t ha}^{-1} \text{ year}^{-1}$ (Almouctar et al. 2021).

Previous studies found the increasing trends of soil loss due to LULC dynamics in various parts of the country (Moges and Bhat 2017; Gashaw et al. 2019; Chimdess et al. 2018). In Ethiopia, the generated average soil losses of Zoa watershed ($20\text{--}41 \text{ t ha}^{-1} \text{ year}^{-1}$) were analogous to $30.6 \text{ t ha}^{-1} \text{ year}^{-1}$ in the Jabi Tehinan district (Amsalu and Mengaw 2014), $31.7 \text{ t ha}^{-1} \text{ year}^{-1}$ in Tiro Afeta and Dedo districts (Gemetchu 2016), $27.5 \text{ t ha}^{-1} \text{ year}^{-1}$ in Upper Blue Nile basin (Haregeweyn et al. 2017), $25 \text{ t ha}^{-1} \text{ year}^{-1}$ in the Agewmariyam catchment (Girmay et al. 2020), and $31 \text{ t ha}^{-1} \text{ year}^{-1}$ in Welmel catchment (Tessema et al. 2020). On the other hand, the quantified soil loss of Zoa watershed was larger than the maximum tolerable soil loss range ($2\text{--}18 \text{ t ha}^{-1} \text{ year}^{-1}$) of the diverse agroecological belts and ($10 \text{ t ha}^{-1} \text{ year}^{-1}$) the northern Ethiopian highlands (Yesuph and Dagnev 2019). On the contrary, some scholars quantified relatively lower soil losses in their studies (Gizachew 2015; Bekele et al. 2019; Bekele and Gemi 2020) and some studies reported higher soil losses (Gelagy and Minale 2016; Belayneh et al. 2019; Girma and Gebre 2020; Mengie et al. 2022). Therefore, the disparity in the estimated soil losses registered was because of the LULC dynamics considered for each study in Ethiopia (Kidane et al. 2019).

The primary factors affecting soil erosion and its severity within the watershed were each LULC dynamics in space and time. Consequently, in 1985, farmland comprised 29.09% of the watershed, and it produced $27.08 \text{ t ha}^{-1} \text{ year}^{-1}$. Later, due to socioeconomic factors, the area of farmland increased to 71.12%, and it generated $59.91 \text{ t ha}^{-1} \text{ year}^{-1}$. Correspondingly, soil loss was higher in farmland and lower in forest areas in the country and elsewhere (Haregeweyn et al. 2017; Belayneh et al. 2019; Kidane et al. 2019; Gashaw et al. 2019; Kulimushi et al. 2021a). In addition, the study conducted by Aneseyee et al. (2020) confirmed that soil erosion increased due to the increasing trend of cultivation in space and time. Likewise, about 1.7% of bareland contributed $31.73 \text{ t ha}^{-1} \text{ year}^{-1}$ in 1985 and its area was expanded to 6.89% and bred soil loss in bareland was about $35.52 \text{ t ha}^{-1} \text{ year}^{-1}$ due to the decreasing rate ($-0.77\% \text{ year}^{-1}$) of forests in the watershed. In comparison to this study, Haregeweyn et al. (2017) estimated soil loss from bare

areas was twice as high. Farmland and bare land are therefore designated as having a high susceptibility to soil erosion and are given priority for effective conservation planning. Our findings also showed that at a watershed outlet, sediment yields rose at the fastest rate, from 39.3% in 1985 to 94.26% in 2021 due to LULC dynamics (Fig. 10). The escalation of temporal sediment yield in the study area from 1985 to 2021 is mainly due to the expansion of farmland and bareland and dwindling of shrubland, grassland and forest area. This situation is impending in the bottom watershed and reservoirs (Gibe III and Gibe IV dams) if not suitable land management is executed in the watershed. Likewise, Haregeweyn et al. (2017) revealed that the life of the GERD dam itself will be endangered by the extreme sedimentation proportion unless appropriate land use planning and SWC practices are applied in the upstream basin to reduce the future impacts of soil erosion and sediment yields.

Soil loss variation across agroecologies and slope gradients

The variations in the soil loss rate are attributed to the varying type of agroecologies and terrain factors in the different parts of Ethiopia and thus one cannot expect agreement while the biophysical and socioeconomic issues in various areas are not the same (Girmay et al. 2020). Due to diverse land use variations in the Zoa watershed, we found that the lowland (Kolla) agroecology had the highest mean soil loss likely attributable to the large bareland coverage with diverse *LS*-factor which require priority management, followed by the midland, and the highland (Fig. 8a). The poor surface cover could result for overgrazing and forest degradation (Berihun et al. 2019; Fenta et al. 2021). On the contrary, Haregeweyn et al. (2017) observed the maximum soil loss from four *Dega* classes or highlands, which contributed 76.6% of the overall soil loss of the area. The synergy of topographic nature in various land use types determines the soil loss and its severity in space and time. The temporal soil loss hazard was increasing with slope gradients in our study area (Fig. 8b). This is triggered by LULC change in relentless topographic features. The quantified spatial soil loss from the northwestern (high bareland proportion), southeastern, and northwestern (large farmland share) parts of the watershed was higher than southern and east-northern margins. Identified erosion susceptible area requires reducing marginal area cultivation toward steep slopes. Correspondingly, previous studies confirmed similar results that soil loss was rising with slope gradients (Amsalu and Mengaw 2014; Haregeweyn et al. 2017; Belayneh et al. 2019). Moreover, Yesuph and Dagnev (2019) reported in the Beshillo catchment of the Blue Nile Basin with slope categories $>60\%$ generates soil

loss ranging from 91 to 935 t ha⁻¹ year⁻¹. Likewise, Hargeweyn et al. (2017) found comparable results, i.e., 77.3% of the watershed generated moderate to very severe erosion from steep slopes.

Conclusion

Quantifying soil loss and its magnitude are contingent on the different land use susceptibility of the soils to erosion, microclimate, general terrain features, and variations in agroecological settings. Therefore, we quantified the impacts of spatiotemporal LULC changes on soil loss across agroecologies and slope categories using a synergy of geospatial technologies and the RUSLE model in Zoa watershed, southwest Ethiopia. The unmanageable changes in land use may impact soil loss, on-site crop productivity, and off-site sediment yields. The extent of spatial and temporal mean annual soil loss varied in the watershed due to the existence of LULC changes. In comparison, soil loss generated from farmland was considered a highly prone area to soil erosion. The spatial soil loss rates of the watershed were wide-ranging and attributed to different land use changes, soil types, and topographic factors. Consequently, the northwest and eastern parts of the watershed lost soil above intolerable levels and it was somewhat extended toward the central and south parts of the watershed. The temporal soil losses were increased during the study periods. The anticipated upsurge in soil loss will reduce land productivity and will negatively affect the livelihood of the host community in the future. In contrast, temporal soil loss experienced from the farmland land use class was the highest, due to an extensive area of grassland and shrubland being transformed into farmland with a conversion rate of 250.74 ha (0.58%) and 448.85 ha (1.05%) per annum, respectively.

Among agroecologies, the highest soil loss was quantified from lowland agroecology. This is might be attributed to lowland area being mainly covered by the land use type of bareland which accelerate soil erosion hazards. The result revealed that soil loss hazard is increasing with slope gradients. Among the reflexive delineated sub-watersheds, the spatiotemporal mean soil loss fell as very severe (>50 t ha⁻¹ year⁻¹) was observed in five sub-watersheds, which accounted for 69% of the area and are required as a high priority for land use and conservation planning. At the watershed outlet, where sediment yield tendencies exceeded at the fastest rate from 39.3% in 1985 to 94.26% in 2021, the rise was the highest. The Gibe III and IV reservoirs, in particular, are at risk of being lost because of the eutrophication and excessive sedimentation brought on by these sediment yields.

RUSLE fails to take the effects of gully erosion and dispersive soils into consideration (Yesuph and Dagnev 2019). Hence, for a more inclusive record of the erosion

hotspot area, identification and measurement of gullies in the watershed should be carried out to improve the accuracy of soil loss determination for better conservation planning and implementation in the future. Moreover, further assessment of the soil conservation fitness, deforestation rates on soil loss, and sediment yields should be carried out to halt soil loss and ensure proper soil management practices.

Therefore, this study suggests that an intensive effort toward increasing forest cover should be executed to reduce the expected upsurge of soil loss and sediment yield in the watershed. Moreover, suitable design of soil and water conservation measures should be implemented considering the terrain features, agroecologies, LULC types, and host community interests. Furthermore, integrated watershed management, agroforestry, soil bund, and terracing should be integrated to manage erosion hotspot areas of very steep terrains and to reduce future soil loss in the watershed. Moreover, since there is no land use policy in the country, very steep slope areas are also used for farmland which exacerbated soil loss. Thus, we recommend that the concerned body should formulate and implement land use policy through community participation.

Acknowledgements

We would like to thank Bonga University and the University of Gondar for their provision to the corresponding author who is a Ph.D. candidate. We also thank the Ethiopian Geospatial Information Agency (EGIA) for providing important geospatial data for this study. Our heartfelt thanks go to the residents of the Zoa watershed in the Dawuro zone and stakeholders for their sharing vital data and experiences.

Author contributions

GG designed and conceived the study, collected and analyzed data, interpreted the findings, and prepared the manuscript. MT, MK, and MJ have contributed to supervising the research, directing and suggesting ideas in the manuscript preparation process. All authors reviewed and approved the final manuscript.

Funding

Not applicable.

Availability of data and materials

The data sets used and analyzed during this study are available from the corresponding author on reasonable request.

Declarations

Ethics approval and consent to participate

Not applicable.

Consent for publication

All authors agreed and approved the manuscript for publication in *Ecological Processes*.

Competing interests

The authors declare that they have no competing interests.

Author details

¹Department of Geography and Environmental Studies, University of Gondar, P.O. Box 196, Gondar, Ethiopia. ²Department of Geography and Environmental Studies, Debre Tabor University, P.O. Box 272, Debre Tabor, Ethiopia.

³Department of Soil Science and Microbiology, Poznan University of Life Sciences, Ul. Szydlowska 50, 60-656 Poznan, Poland.

Received: 1 December 2022 Accepted: 2 May 2023

Published online: 22 May 2023

References

- Adimassu Z, Mekonnen K, Yirga C, Kessler A (2014) Effect of soil bunds on runoff, soil and nutrient losses, and crop yield in the central highlands of Ethiopia. *Land Degrad Dev* 25(6):554–564
- Aduagna A, Abegaz A, Cerda A (2015) Soil erosion assessment and control in Northeast Wollega, Ethiopia. *Solid Earth Discuss* 7(4):3511–3540
- Agidew AMA, Singh KN (2017) The implications of land use and land cover changes for rural household food insecurity in the Northeastern highlands of Ethiopia: the case of the Teleyayen sub-watershed. *Agric Food Secur* 6:1–14
- Alewell C, Borelli P, Meusburger K, Panagos P (2019) Using the USLE: chances, challenges and limitations of soil erosion modeling. *Int Soil Water Conserv Res* 7:203–225
- Almouctar MA, Wu Y, Zhao F, Dossou JF (2021) Soil erosion assessment using the RUSLE model and geospatial techniques (Remote Sensing and GIS) in South-Central Niger (Maradi Region). *Water* 13(24):3511
- Amellah O, Morabiti K (2021) Assessment of soil erosion risk severity using GIS, remote sensing and RUSLE model in Oued Laou Basin (north Morocco). *Soil Sci Annu* 72(3):142530
- Amsalu T, Mengaw A (2014) GIS based soil loss estimation using RUSLE model: the case of Jabi Tehinan Woreda, ANRS, Ethiopia. *Natural Resour* 5:616–626
- Aneseyee AB, Soromessa T, Elias E (2020) The effect of land use/land cover changes on ecosystem services valuation of Winike watershed, Omo Gibe basin, Ethiopia. *Hum Ecol Risk Assess* 26(10):2608–2627
- Atoma H, Suryabhadgavan KV, Balakrishnan M (2020) Soil erosion assessment using RUSLE model and GIS in Huluka watershed, Central Ethiopia. *Sustain Water Resour Manage* 6(1):12
- Barriuso Mediavilla A, Salas Tovar E, Bosque González ID (2017) GIS model for potential soil erosion with the optimization of RUSLE equation. Case of study: olive oil PDO in Aragón and Andalucía Regions (Spain). *Agile: Wageningen, The Netherlands*. pp 9–12
- Bekele B, Muluneh A, Wondrade N (2019) Geographic Information System (GIS) based soil loss estimation using Universal Soil Loss Equation Model (USLE) for soil conservation planning in Karesa Watershed, Dawuro Zone, South West Ethiopia. *Int J Water Resour Environ Eng* 11(8):143–158
- Bekele B, Gerni Y (2020) Soil erosion risk and sediment yield assessment with universal soil loss equation and GIS: in Dijo watershed, Rift valley Basin of Ethiopia. *Model Earth Syst Environ* 7:273–291
- Belay T, Mengistu DA (2019) Land use and land cover dynamics and drivers in the Muga watershed, Upper Blue Nile basin, Ethiopia. *Remote Sens Appl Soc Environ* 15:100249
- Belay T, Mengistu DA (2021) Impacts of land use/land cover and climate changes on soil erosion in Muga watershed, Upper Blue Nile basin (Abay), Ethiopia. *Ecol Process* 10:68
- Belayneh M, Yirgu T, Tsegaye D (2019) Potential soil erosion estimation and area prioritization for better conservation planning in Gumara watershed using RUSLE and GIS techniques. *Environ Syst Res* 8(1):20
- Belete M, Deng J, Abubakar GA, Teshome M, Wang K, Woldetsadik M, et al (2020) Partitioning the impacts of land use/land cover change and climate variability on water supply over the source region of the Blue Nile Basin. *Land Degrad Dev* 31(15):2168–2184
- Berihun ML, Tsunekawa A, Haregeweyn N, Meshesha DT, Adgo E, Tsubo M et al (2019) Exploring land use/land cover changes, drivers and their implications in contrasting agro-ecological environments of Ethiopia. *Land Use Policy* 87:104052
- Betru T, Tolera M, Sahle K, Kassa H (2019) Trends and drivers of land use/land cover change in Western Ethiopia. *Appl Geogr* 104:83–93
- Biswas S (2012) Estimation of soil erosion using remote sensing and GIS and prioritization of catchments. *Int J Emerg Technol Adv Eng* 2(7):124
- Borrelli P, Lugato E, Montanarella L, Panagos P (2017) A new assessment of soil loss due to wind erosion in European agricultural soils using a quantitative spatially distributed modelling approach. *Land Degrad Dev* 28(1):335–344
- Bullock EL, Healey SP, Yang Z, Oduor P, Gorelick N, Omondi S et al (2021) Three decades of land cover change in East Africa. *Land* 10(2):150
- Chang TJ, Zhou H, Guan Y (2016) Applications of erosion hotspots for watershed investigation in the Appalachian Hills of the United States. *J Irrig Drain Eng* 142:04015057
- Chen D, Stow D (2002) The effect of training strategies on supervised classification at different spatial resolution. *J Photogramm Eng Remote Sens* 68(11):1155–1162
- Chimdessa K, Quraishi S, Kebede A, Alamirew T (2018) Effect of land use land cover and climate change on river flow and soil loss in Didessa River Basin, South West Blue Nile, Ethiopia. *Hydrology* 6(1):2
- Debie E (2021) Smallholder farmers' decisions to the combined use of soil conservation practices in Tiwa watershed, Northwest Highlands of Ethiopia. *Heliyon* 7(1):e05958
- Degjife A, Worku H, Gizaw S, Legesse A (2019) Land use land cover dynamics, its drivers and environmental implications in Lake Hawassa Watershed of Ethiopia. *Remote Sens Appl Soc Environ* 14:178–190
- Dibaba WT, Demissie TA, Miegel K (2020) Drivers and implications of land use/land cover dynamics in Finchaa Catchment, Northwestern Ethiopia. *Land* 9(4):1–20
- Dinka MO (2020) Quantification of soil erosion and sediment yield for ungauged catchment using the RUSLE model: case study for Lake Basaka catchment in Ethiopia. *Lakes Reserv Res Manag* 25(2):183–195
- Ewunetu A, Simane B, Teferi E, Zaitchik BF (2021) Land cover change in the Blue Nile River headwaters: farmers' perceptions, pressures, and satellite-based mapping. *Land* 10(1):68
- FAO (1986) Ethiopian Highland Reclamation Study, Final Report. FAO: Rome, Italy. pp 37–46
- Farhan Y, Zregat D, Farhan I (2013) Spatial estimation of soil erosion risk using RUSLE approach, RS, and GIS techniques: a case study of Kufranja watershed, Northern Jordan. *J Water Resour Prot* 5(12):1247
- Fenta AA, Tsunekawa A, Haregeweyn N, Poesen J, Tsubo M, Borrelli P, Kurosaki Y (2020) Land susceptibility to water and wind erosion risks in the East Africa region. *Sci Total Environ* 703:135016
- Fenta AA, Tsunekawa A, Haregeweyn N, Tsubo M, Yasuda H, Kawai T, Ebabu K, Berihun ML, Belay AS, Sultan D (2021) Agroecology-based soil erosion assessment for better conservation planning in Ethiopian river basins. *Environ Res* 195:110786
- Gashaw T, Tulu T, Argaw M, Worqlul AW (2018) Modeling the hydrological impacts of land use/land cover changes in the Andassa watershed, Blue Nile Basin, Ethiopia. *Sci Total Environ* 619:1394–1408
- Gashaw T, Tulu T, Argaw M, Worqlul AW (2019) Modeling the impacts of land use–land cover changes on soil erosion and sediment yield in the Andassa watershed, upper Blue Nile basin, Ethiopia. *Environ Earth Sci* 78(24):679
- Gashaw T, Worqlul AW, Dile YT, Addisu S, Bantider A, Zeleke G (2020) Evaluating potential impacts of land management practices on soil erosion in the Gilgel Abay watershed, upper Blue Nile basin. *Heliyon* 6(8):e04777
- Gebre GG, Isoda H, Amekawa Y, Nomura H (2021) Gender differences in agricultural productivity: evidence from maize farm households in southern Ethiopia. *GeoJournal* 86:843–864
- Gelagay HS, Minalé AS (2016) Soil loss estimation using GIS and Remote sensing techniques: A case of Koga watershed, Northwestern Ethiopia. *Int Soil Water Conserv Res* 4:126–136
- Gemechu A (2016) Estimation of soil loss using revised universal soil loss equation and determinants of soil loss in Tiro Afeta and Dedo Districts of Jimma Zone, Oromiya National Regional State, Ethiopia. *Trends Agric Econ* 9(1):1–12
- Gessesse AA, Melesse AM, Abiy AZ (2019) Land use dynamics and base and peak flow responses in the Choke mountain range, Upper Blue Nile Basin, Ethiopia. *Int J River Basin Manage* 19(1):109–121
- Girma R, Gebre E (2020) Spatial modeling of erosion hotspots using GIS-RUSLE interface in Omo-Gibe River basin, Southern Ethiopia: implication for soil and water conservation planning. *Environ Syst Res* 9:19

- Girmay G, Moges A, Muluneh A (2020) Estimation of soil loss rate using the USLE model for Agewmariyam Watershed, northern Ethiopia. *Agric Food Secur* 9(1):1–12
- Gitima G, Legesse A, Biru D (2021) Assessing the impacts of climate variability on rural households in agricultural land through the application of livelihood vulnerability index. *Geosfera Indonesia* 6(1):96–126. <https://doi.org/10.19184/geosi.v6i1.20718>
- Gitima G, Teshome M, Kassie M, Jakubus M (2022) Spatiotemporal land use and cover changes across agroecologies and slope gradients using geospatial technologies in Zoa watershed, Southwest Ethiopia. *Heliyon* 8(9):e10696
- Gizachew A (2015) A geographic information system-based soil loss and sediment estimation in Zingini watershed for conservation planning, highlands of Ethiopia. *World Appl Sci J* 33(1):69–79
- Hailu A, Mammo S, Kidane M (2020) Dynamics of land use, land cover change trend and its drivers in Jimma Geneti District, Western Ethiopia. *Land Use Policy* 99:105011
- Han J, Ge W, Hei Z, Cong C, Ma C, Xie M, Liu B, Feng W, Wang F, Jiao J (2020) Agricultural land use and management weaken the soil erosion induced by extreme rainstorms. *Agric Ecosyst Environ* 301:107047
- Haregeweyn N, Tsunekawa A, Poesen J, Tsubo M, Meshesha DT, Fenta AA et al (2017) Comprehensive assessment of soil erosion risk for better land use planning in river basins: case study of the Upper Blue Nile River. *Sci Total Environ* 574:95–108
- Hurni H (1985) Erosion-productivity-conservation systems in Ethiopia. In: Plasentis I ed. *Soil Conservation and Productivity. Proceedings IV International Conference on soil conservation, Maracay, Venezuela.* <https://boris.unibe.ch/77547/>
- Hurni H, Herweg K, Portner B, Liniger H (2008) Soil erosion and conservation in global agriculture. In: *Land use and soil resources.* Springer, Dordrecht, pp 41–71
- Karamage F, Zhang C, Kayiranga A, Shao H, Fang X, Ndayisaba F et al (2016) USLE-based assessment of soil erosion by water in the Nyabarongo River Catchment, Rwanda. *Int J Environ Res Public Health* 13(8):835
- Kidane M, Bezie A, Kesete N, Tolessa T (2019) The impact of land use and land cover (LULC) dynamics on soil erosion and sediment yield in Ethiopia. *Heliyon* 5(12):e02981
- Kijowska-Strugała M, Bucala-Hrabia A, Demczuk P (2018) Long-term impact of land use changes on soil erosion in an agricultural catchment (in the Western Polish Carpathians). *Land Degrad Dev* 29(6):1871–1884
- Kulimushi LC, Choudhari P, Mubalama LK, Banswe GT (2021a) GIS and remote sensing-based assessment of soil erosion risk using RUSLE model in South-Kivu province, eastern, Democratic Republic of Congo. *Geomat Nat Haz Risk* 12(1):961–987
- Kulimushi LC, Maniragaba A, Choudhari P, Elbeltagi A, Uwemeye J, Rushema E, Singh SK (2021b) Evaluation of soil erosion and sediment yield spatio-temporal pattern during 1990–2019. *Geomat Nat Haz Risk* 12(1):2676–2707
- Legese KG, Gelanew A (2019) Soil degradation extent and dynamics of soil fertility improvement technologies in Majete Watershed, North Ethiopia. *J Soil Sci Environ Manage* 10(3):39–45
- León JD, Osorio NW (2014) Role of litter turnover in soil quality in tropical degraded lands of Colombia. *Sci World J* 2014:693981
- Lin J, Guan Q, Tian J, Wang Q, Tan Z, Li Z, Wang N (2020) Assessing temporal trends of soil erosion and sediment redistribution in the Hexi Corridor region using the integrated RUSLE-TLSD model. *Catena* 195:104756
- Ly S, Charles C, Degre A (2013) Different methods for spatial interpolation of rainfall data for operational hydrology and hydrological modeling at watershed scale: a review. *Biotechnol Agron Soc Environ* 17(2):392–406
- Mengie MA, Hagos YG, Maleda DA, Andualem TG (2022) Assessment of soil loss rate using GIS-RUSLE interface in Tashat Watershed, Northwestern Ethiopia. *J Sediment Environ* 7(3):617–631
- Messay M (2011) Land-use/land-cover dynamics in Nonno district, Central Ethiopia. *J Sustain Dev Africa* 13:123–139
- Ministry of Agriculture (MOA) (1998) *Agro Ecological Zones of Ethiopia.* MOA, Addis Ababa, Ethiopia
- Minta M, Kibret K, Thorne P, Nigussie T, Nigatu L (2018) Land use and land cover dynamics in Dendi-Jeldu hilly-mountainous areas in the central Ethiopian highlands. *Geoderma* 314:27–36
- Moges DM, Bhat HG (2017) Integration of geospatial technologies with RUSLE for analysis of land use/cover change impact on soil erosion: case study in Rib watershed, north-western highland Ethiopia. *Environ Earth Sci* 76(22):765
- Molla T, Sisseber B (2017) Estimating soil erosion risk and evaluating erosion control measures for soil conservation planning at Koga watershed in the highlands of Ethiopia. *Solid Earth* 8(1):13–25
- Nehai SA, Guettouche MS (2020) Soil loss estimation using the revised universal soil loss equation and a GIS-based model: a case study of Jijel Wilaya, Algeria. *Arabian J Geosci* 13(4):152
- Nguyen XH, Pham AH (2018) Assessing soil erosion by agricultural and forestry production and proposing solutions to mitigate: a case study in Son La Province, Vietnam. *Appl Environ Soil Sci* 2018:2397265
- Nkonya E, Mirzabaev A, Von Braun J (2016) *Economics of land degradation and improvement—a global assessment for sustainable development.* Springer Nature, Berlin, p 686
- Ogato GS, Bantider A, Geneletti D (2021) Dynamics of land use and land cover changes in Huluka watershed of Oromia Regional State, Ethiopia. *Environ Syst Res* 10:10
- Pan J, Wen Y (2014) Estimation of soil erosion using RUSLE in Caijiamiao watershed, China. *Nat Hazards* 71(3):2187–2205
- Pimentel D, Harvey C, Resosudarmo P, Sinclair K, Kurz D, McNair M et al (1995) Environmental and economic costs of soil erosion and conservation benefits. *Science* 267(5201):1117–1123
- Potapov P, Hansen M C, Pickens A, Hernandez-Serna A, Tyukavina A, Turubanova S et al (2022) The global 2000–2020 land cover and land use change dataset derived from the Landsat archive: first results. *Front Remote Sens* 18:1–22
- Renard KG, Laflen JM, Foster GR, McCool DK (1994) The revised universal soil loss equation. *Soil Erosion Res Methods* 2:105–124
- Renard KG, Foster GR, Weesies GA, McCool DK, and Yoder DC (1997) Predicting soil erosion by water: a guide to conservation planning with the Revised Universal Soil Loss Equation (RUSLE). *Agriculture Handbook No. 703*
- Sheikh AH, Palria S, Alam A (2011) Integration of GIS and universal soil loss equation (USLE) for soil loss estimation in a Himalayan watershed. *Recent Res Sci Technol* 3(3):51–57
- Sisay G, Gitima G, Mersha M, Alemu WG (2021) Assessment of land use land cover dynamics and its drivers in Bechet Watershed Upper Blue Nile Basin, Ethiopia. *Remote Sens Appl Soc Environ* 24:100648
- Tadesse L, Suryabhagavan KV, Sridhar G, Legesse G (2017) Land use and land cover changes and soil erosion in Yezaat Watershed, North Western Ethiopia. *Int Soil Water Conserv Res* 5(2):85–94
- Tebebu TY, Abiy AZ, Zegeye AD, Dahlke HE, Easton ZM, Tilahun SA et al (2010) Surface and subsurface flow effect on permanent gully formation and upland erosion near Lake Tana in the northern highlands of Ethiopia. *Hydrol Earth Syst Sci* 14(11):2207–2217
- Tewabe D, Fentahun T (2020) Assessing land use and land cover change detection using remote sensing in the Lake Tana Basin, Northwest Ethiopia Assessing land use and land cover change detection using remote sensing in the Lake Tana Basin, Northwest Ethiopia. *Cogent Environ Sci* 6(1). <https://doi.org/10.1080/23311843.2020.1778998>
- Teng HF, Liang ZZ, Chen SC, Yu W, Viscarra Rossel RA, Chappell A, Shi Z (2018) Current and future assessments of soil erosion by water on the Tibetan Plateau based on RUSLE and CMIP5 climate models. *Sci Total Environ* 635:673–686
- Tesfahunegn GB, Tamene L, Vlek PL (2014) Soil erosion prediction using Morgan-Morgan-Finney model in a GIS environment in Northern Ethiopia catchment. *Appl Environ Soil Sci* 2014:1–15
- Tesfaye G, Tibebe D (2018) Soil erosion modeling using GIS based RUSLE model in Gilgel Gibe-1 catchment, South West Ethiopia. *Int J Environ Sci Natural Resour* 15(5):141–148
- Tessema YM, Jasińska J, Yadeta LT, Świtoniak M, Puchalka R, Gebregeorgis EG (2020) Soil loss estimation for conservation planning in the wemel watershed of the Genale Dawa Basin, Ethiopia. *Agronomy* 10(6):777
- Tolessa T, Dechassa C, Simane B, Alamerew B, Kidane M (2020) Land use/land cover dynamics in response to various driving forces in Didessa sub-basin, Ethiopia. *Geojournal* 85(3):747–760
- Tsegaye B (2019) Effect of land use and land cover changes on soil erosion in Ethiopia. *Int J Agric Sci Food Technol* 5(1):26–34

- Williams JR, Berndt HD (1977) Sediment yield prediction based on watershed hydrology. *Trans ASAE* 20:1100–1104
- Wischmeier WH, Smith DD (1978) Predicting rainfall erosion losses: a guide to conservation planning (No. 537). Science and Education Administration, United States Department of Agriculture, Washington DC
- Woldemariam WG, Harka EA (2020) Effect of land use and land cover change on soil erosion in Erer sub-basin, Northeast Wabi Shebelle Basin, Ethiopia. *Land* 9(4):111
- Wynants M, Kelly C, Mtei K, Munishi L, Patrick A, Rabinovich A et al (2019) Drivers of increased soil erosion in East Africa's agro-pastoral systems: changing interactions between the social, economic and natural domains. *Regional Environ Change* 19(7):1909–1921
- Yahya F, Zregat D, Farhan I (2013) Spatial estimation of soil erosion risk using RUSLE approach, RS, and GIS techniques: a case study of Kufranja Watershed, Northern Jordan. *J Water Resour Prot* 5:1247–1261
- Yesuph AY, Dagne AB (2019) Soil erosion mapping and severity analysis based on RUSLE model and local perception in the Beshillo Catchment of the Blue Nile Basin, Ethiopia. *Environ Syst Res* 8(1):17
- Yiferu Y, Taddese G, Mebrate T (2018) Influence of soil erosion and conservation practices on soil physical properties in Ginaberet, Ethiopia. *For Res Eng Int J* 2:288–297
- Zerihun M, Mohammedyasin MS, Sewnet D, Adem AA, Lakew M (2018) Assessment of soil erosion using RUSLE, GIS and remote sensing in NW Ethiopia. *Geoderma Reg* 12:83–90
- Zhang H, Yang Q, Li R, Liu Q, Moore D, He P et al (2013) Extension of a GIS procedure for calculating the RUSLE equation LS factor. *Comput Geosci* 52:177–188
- Zhang S, Fan W, Li Y, Yi Y (2017) The influence of changes in land use and landscape patterns on soil erosion in a watershed. *Sci Total Environ* 574:34–45

Publisher's Note

Springer Nature remains neutral with regard to jurisdictional claims in published maps and institutional affiliations.

Submit your manuscript to a SpringerOpen[®] journal and benefit from:

- Convenient online submission
- Rigorous peer review
- Open access: articles freely available online
- High visibility within the field
- Retaining the copyright to your article

Submit your next manuscript at ► [springeropen.com](https://www.springeropen.com)
